JOURNAL OF GEOPHYSICAL RESEARCH, VOL. 111, D12306, doi:10.1029/2005JD006354, 2006

Effects of changing power plant NO_x emissions on ozone in the eastern United States: Proof of concept

G. J. Frost,[1,2] S. A. McKeen,[1,2] M. Trainer,[1] T. B. Ryerson,[1] J. A. Neuman,[1,2] J. M. Roberts,[1] A. Swanson,[1,2] J. S. Holloway,[1,2] D. T. Sueper,[1,2] T. Fortin,[1,2] D. D. Parrish,[1] F. C. Fehsenfeld,[1,2] F. Flocke,[3] S. E. Peckham,[2,4] G. A. Grell,[2,4] D. Kowal,[5] J. Cartwright,[5] N. Auerbach,[5] and T. Habermann[5]

Received 10 June 2005; revised 20 January 2006; accepted 17 February 2006; published 20 June 2006.

[1] Recent decreases in nitrogen oxide (NO_x = NO + NO_2) emissions from eastern U.S. power plants and their effects on regional ozone are studied. Using the EPA 1999 National Emission Inventory as a reference emission data set, NO_x and sulfur dioxide (SO_2) emission rates at selected power plants are updated to their summer 2003 levels using Continuous Emission Monitoring System (CEMS) measurements. The validity of the CEMS data is established by comparison to observations made on the NOAA WP-3 aircraft as part of the 2004 New England Air Quality Study. The impacts of power plant NO_x emission decreases on O_3 are investigated using the WRF-Chem regional chemical forecast model. Summertime NO_x emission rates decreased by approximately 50% between 1999 and 2003 at the subset of power plants studied. The impact of NO_x emission reductions on ozone was moderate during summer 2004 because of relatively cool temperatures and frequent synoptic disturbances. Effects in individual plant plumes vary depending on the plant's NO_x emission strength, the proximity of other NO_x sources, and the availability of volatile organic compounds (VOCs) and sunlight. This study provides insight into the ozone changes that can be anticipated as power plant NO_x emission reductions continue to be implemented throughout the United States.

Citation: Frost, G. J., et al. (2006), Effects of changing power plant NO_x emissions on ozone in the eastern United States: Proof of concept, *J. Geophys. Res.*, *111*, D12306, doi:10.1029/2005JD006354.

1. Introduction

[2] U.S. electric power generation accounted for approximately one quarter of national NO_x emissions and two thirds of national SO_2 emissions in 1999 (http://www.epa.gov/ttn/chief/trends/index.html). NO_x emissions, in combination with VOCs, sunlight, and warm temperatures, lead to the production of ozone, the primary component of photochemical smog. SO_2 and NO_x emissions are linked to acid deposition and precipitation and to atmospheric particulate formation.

[3] Actions taken by the federal and state governments working in collaboration with the electric power industry have reduced NO_x emissions from U.S. power plants during recent years [*U.S. Environmental Protection Agency* (*U.S. EPA*), 2003, 2004a, 2004b]. Title IV of the 1990 Clean Air Act Amendments (CAAA) established the Acid Rain Program (ARP), which set limitations on annual NO_x emission rates (NO_x mass emissions per unit of heat input to the boiler) at U.S. coal-fired power plants (http://www.epa.gov/airmarkets/arp/regs/index.html). From 1990 to 2000, annual NO_x emissions from electric utility units affected by the ARP dropped by 18%, and actual 2000 NO_x emissions for these units were 3 million tons less than the projected level had Title IV not taken effect [*U.S. EPA*, 2003]. The 1990 CAAA also established the Ozone Transport Commission (OTC), whose cap-and-trade NO_x Budget Program achieved NO_x emission reductions from sources in 11 northeast states and the District of Columbia (DC) during the ozone seasons (May through September) of 1999 through 2002. Ozone Transport and Assessment Group analyses led to the 1998 NO_x State Implementation Plan (SIP) Call by the U.S. Environmental Protection Agency (EPA). The rule concluded that NO_x emissions from 22 eastern states and DC contribute to ozone nonattainment in the eastern United States and required the states to amend SIPs and limit NO_x emissions. The EPA set an ozone season NO_x budget for each affected state that capped NO_x emissions, with 2003 as the first control year. The rule did not mandate which sources must reduce emissions, but required states to meet an overall cap and gave states flexibility to design control strategies. The current NO_x

[1]Chemical Sciences Division, Earth System Research Laboratory, NOAA, Boulder, Colorado, USA.
[2]Also at Cooperative Institute for Research in Environmental Sciences, University of Colorado, Boulder, Colorado, USA.
[3]Atmospheric Chemistry Division, National Center for Atmospheric Research, Boulder, Colorado, USA.
[4]Global Systems Division, Earth System Research Laboratory, NOAA, Boulder, Colorado, USA.
[5]NOAA National Geophysical Data Center, Boulder, Colorado, USA.

0148-0227/06/2005JD006354$09.00

Budget Trading Program (NBP), which extends the earlier OTC program to the above 22 states and DC, is a cap-and-trade program for large electric generating units and large industrial boilers, turbines and combined cycle units. By 2003 the entire NBP area had reduced point source NO_x emissions by more than 50% below 1990 baseline levels and by about a third below 2000 levels. These reductions represent the combined effects of limitations set by the ARP, the OTC NO_x Budget Program, the NBP, and other CAAA and state-required controls [*U.S. EPA*, 2004b]. Significant power plant NO_x emission reductions are expected to continue as the entire NBP area comes in to compliance with the NO_x SIP Call. These controls have reduced the amount of NO_x emitted per unit of power produced despite an increase in the electric power generated by U.S. plants [*U.S. EPA*, 2004b].

[4] Electric utilities can choose from many options to comply with the above programs [*U.S. EPA*, 2004b]. Plants can shift power generation from higher NO_x-emitting units to less polluting ones. Many plants use low-NO_x burner and overfire air technologies to reduce NO_x formation from nitrogen present in boiler combustion air and fuel. NO_x emissions can also be limited using add-on controls, such as selective catalytic reduction (SCR) or selective noncatalytic reduction (SNCR). These controls use injected ammonia in the flue gas within or downstream from the combustion unit to react with NO_x and form N_2 and water. SCR uses a catalyst to improve efficiency and to allow lower temperature combustion. Reburning, where gas or coal is injected downstream of the primary combustion zone to further remove NO_x, can also be used to increase control efficiency. Finally, the NBP allows utility companies to purchase emission allowances from other market participants.

[5] Most U.S. power plants, including those accounting for 96% of ozone season NO_x emissions in the states composing the NBP, use a Continuous Emission Monitoring System (CEMS) to monitor and record emissions [*U.S. EPA*, 2004b]. A CEMS directly measures flue gas NO_x and SO_2 concentrations as well as heat input to calculate the NO_x emission rate on an ongoing basis. The CEMS data for all ARP units are reported every calendar quarter to the EPA and are available in either quarterly summaries or hourly format on EPA's Clean Air Markets web site, http://www.epa.gov/airmarkets/emissions.

[6] CEMS direct measurements of criteria pollutants represent one of the most accurate parts of the U.S. emissions database. They are incorporated in to the National Emission Inventory (NEI), the principal U.S. air quality modeling EI (http://www.epa.gov/ttn/chief/net/index.html). The EPA constructs a new NEI every 3 years using input from state and local agencies. The latest fully vetted NEI version at this time is 1999 version 3 (NEI99). The multiyear NEI preparation time results from a number of factors, including the lag between CEMS data reporting by electric utilities and the EPA's quality assurance checks on the data, the merging of these data with other NEI inventory components, and the overall complexity of accounting for other source contributions within the complete inventory. Many air quality research model simulations for the last several years rely on the NEI99, which does not capture changes in U.S. power plant emissions since 1999. These models therefore overestimate summer power plant NO_x emissions, which could directly impact subsequent O_3 predictions.

[7] Clear evidence of the impact of power plant NO_x emission reductions on ambient concentrations of nitrogen oxides is elusive. A recent ARP progress report [*U.S. EPA*, 2003] noted that wet nitrate deposition was lower throughout the northeast United States for the average of 2000–2002 compared with the 1989–1991 average, on the basis of observations from the National Atmospheric Deposition Program (NADP). However, lower precipitation levels could explain decreased wet nitrate deposition. There were no significant decreases observed in NADP wet nitrate concentrations between the above two time periods, and mean ambient particulate nitrate concentrations in the eastern United States measured by the Clean Air Status and Trends Network (CASTNET) have remained unchanged or even increased in some areas [*U.S. EPA*, 2003]. Because power plants represent roughly one quarter of U.S. NO_x emissions, the lack of observable ambient impacts from plant emission reductions at the current time is probably not surprising. Indeed, the EPA suggests [*U.S. EPA*, 2003, 2004a] that observable changes in atmospheric concentrations of nitrogen oxides may be expected only after full implementation of the various NO_x control programs during the next decade. *Butler et al.* [2005] find that reducing total NO_x emissions by 50% should decrease total nitrogen deposition at the northeastern U.S. CASTNET sites by about 25%, while a 50% reduction in nonvehicle NO_x emissions would decrease the CASTNET-measured total nitrogen deposition by 15%.

[8] The EPA reports small but significant decreases in O_3 levels in eastern U.S. metropolitan areas since the mid-1990s [*U.S. EPA*, 2004c]. Additionally, the largest reductions in the fourth highest maximum 8-hour O_3 concentrations between 1990 and 2003 in the NBP region occurred in northeast and mid-Atlantic states, which are generally downwind of the power plants with the highest NO_x emissions [*U.S. EPA*, 2004b]. The EPA's ozone standard allows three 8-hour maximum O_3 concentrations of above 84 ppbv in a given area before an exceedance is registered, so the fourth highest maximum concentration statistic gives a measure of an area's compliance with the standard. These O_3 trends coincide temporally with decreases in NO_x due to the Acid Rain Program and seasonal OTC state reductions, suggesting that the air quality improvement may in part be due to power plant NO_x emission reductions [*U.S. EPA*, 2004c]. *Reynolds et al.* [2004] also report significant decreases in the fourth highest 8-hour maximum O_3 in eastern U.S. metropolitan areas between 1980 and 2002 but did not find such trends when restricting data to just the 1992–2002 period.

[9] Further complicating this picture, atmospheric O_3 is affected by trends in NO_x and VOC emission contributions from other sources. The EPA reports reductions in mobile source NO_x and VOC emissions since the mid-1990s (http://www.epa.gov/ttn/chief/trends/index.html). Other analyses suggest that mobile NO_x emissions may have decreased either less quickly than the EPA estimates or may have even increased in the past two decades [*Parrish et al.*, 2002; *Parrish*, 2006; *Harley et al.*, 2005]. These studies illustrate the difficulty in assessing the impact of decreasing power plant NO_x emissions on ozone, given the relative impor-

tance of other NO_x sources and simultaneous NO_x and VOC mobile emission changes in recent years.

[10] The focus of the current work is the impact of recent decreases in power plant NO_x emissions on O_3 concentrations in the eastern United States during the summer of 2004. CEMS quarterly summaries from the summer of 2003 are used to update the NEI99 emission rates of a number of eastern U.S. power plants. Air quality model simulations of O_3 using both the NEI99 and the updated 2003 emission rates are compared. The O_3 response to a unit NO_x emission reduction within individual power plant plumes is a function of the NO_x levels in the plume (resulting from both the plant's own NO_x emissions and those of other nearby sources), biogenic emissions in the vicinity of the plant, and sunlight levels. This work represents a partial assessment of changes in O_3 due to power plant NO_x emission reductions. The current paper serves as a proof of concept for our method of updating power plant emissions and evaluating their impacts, and as such, focuses on general behavior by means of a case study for a summer day in 2004. This is the first of several papers in which we investigate recent emission changes and their impacts on air quality in the eastern United States.

2. Methods

2.1. WP-3 Observations

[11] This work is carried out as a part of the 2004 International Consortium for Atmospheric Research on Transport and Transformation/New England Air Quality Study (ICARTT/NEAQS2K4), http://www.al.noaa.gov/ICARTT/. Observations from the NOAA WP-3 aircraft, while focused on the New England area, include data taken across the eastern United States and southern Canada, from Nova Scotia in the north to Florida in the south and from Georgia and Ohio in the west to about 60 deg W longitude over the North Atlantic Ocean. Of interest to this work are WP-3 measurements of the mixing ratios of NO, NO_2, NO_y (total reactive gas-phase nitrogen = NO_x + HNO_3 + all organic nitrate compounds +...), HNO_3, peroxycarboxylic nitric anhydride (PAN), peroxypropionic nitric anhydride (PPN), peroxymethacrylic nitric anhydride (MPAN), and SO_2 during several flights (25 July and 6, 9, and 15 August 2004) which included downwind transects of eastern U.S. power plant plumes (http://www.al.noaa.gov/2004/p3platform.shtml).

[12] HNO_3 was measured with chemical ionization mass spectrometry (CIMS) [*Neuman et al.*, 2002]. PAN-type compounds were detected using thermal dissociation followed by CIMS detection of acylperoxy radicals [*Slusher et al.*, 2004; *Swanson et al.*, 2004]. SO_2 was measured by UV pulsed fluorescence. NO, NO_2 and NO_y were measured using NO/O_3 chemiluminescence, with photolysis to convert NO_2 to NO and the catalytic conversion of all nitrogen oxides to NO on a hot gold surface in the presence of CO [*Ryerson et al.*, 1999, 2000]. Problems with the NO_y converter led to uncertainties in the conversion fraction beginning with the 15 July flight and progressively worsening during the course of the mission, including all flights of interest indicated above. Because of the uncertainties in measured NO_y, we instead use the sum of measured reactive nitrogen species, NO_{yi},

$$NO_{yi} = NO + NO_2 + HNO_3 + PAN + PPN + MPAN.$$

For the two NEAQS2K4 flights when both the measured NO_y and NO_{yi} are available and reliable, the two sets of data agree to within the combined uncertainties.

[13] Each of these observations was carried out with 1-s time resolution, except PAN, PPN, and MPAN, which were measured at 2-s resolution and then interpolated to the 1-s time base of the other measurements before calculating the NO_{yi} sum. This temporal resolution allowed for ~100 m spatial resolution at typical WP-3 air speeds. These measurements were employed in plume transects downwind from power plants to estimate actual plant emission ratios of SO_2 to NO_x.

2.2. Reference Emission Inventory

[14] The reference model emission inventory was constructed for use by air quality forecast models deployed during ICARTT/NEAQS2K4, with the intention that the EI serve as an interim data set until an official EPA 2004 emission inventory was constructed. Emission processing was carried out using custom-built FORTRAN routines developed at the NOAA Chemical Sciences Division. The basis for the U.S. portion of this inventory is the EPA NEI99 version 3 (http://www.epa.gov/ttn/chief/net/1999inventory.html#final3crit), released in November 2003 and updated with any changes prior to March 2004. Other emission processing data such as spatial surrogates, temporal allocation factors, and chemical speciation profiles were taken from EPA's Clearinghouse for Inventories and Emissions Factors (CHIEF) web site, http://www.epa.gov/ttn/chief/emch/index.html.

[15] Area and mobile source emissions were distributed on a 4-km horizontal resolution Lambert-Conformal grid encompassing the continental United States, southern Canada, and northern Mexico (24–52°N latitude, 60–125°W longitude). U.S. county-level area and mobile emissions were allocated using EPA's spatial surrogates on this grid and an EPA cross reference of these surrogates to the source classification codes (SCCs) of each emission process in the county-level inventory. 1995 Canadian province- and census-division-level area and mobile source emissions obtained from EPA (ftp://ftp.epa.gov/EmisInventory/canada_SMOKE) were spatially allocated using Canadian gridded surrogates in a manner similar to that of the U.S. county-level data. 1999 Mexican state-level area source emissions north of 24°N compiled for the BRAVO study (http://www.epa.gov/ttn/chief/net/mexico.html) were spatially allocated using a 36-km gridded population surrogate and then projected on to the 4-km grid.

[16] U.S. point emissions were reported in the processed EI for discrete sources identified by latitude and longitude and accompanied by stack parameter information to allow for plume-rise calculations. As discussed in the Introduction, 1999 CEMS data are the basis for most U.S. power plant emissions in the NEI99. The CEMS data in the NEI99 are reported as both annual averages and ozone season day (OSD) averages, defined in the NEI99 as the average daily emissions for the period 1 June to 30 August. No Canadian point source information was available because of industry nondisclosure rules. A small number of Mexican point sources from the BRAVO study were included in the processed EI.

[17] The processed EI included emissions of seven primary species (NO_x, CO, VOC, SO_2, NH_3, PM2.5, PM10),

41 speciated VOC compounds, and 5 speciated PM2.5 aerosol components calculated for each hour of an OSD. The large number of VOC species is designed for flexibility in assigning VOC emissions within various lumped photochemical mechanisms. Because this inventory was developed for use during a summer field study, OSD emissions were used to construct the processed EI. If OSD emissions were not reported for a particular source, annual emissions were converted to OSD values using the CHIEF temporal allocation factors, which distribute emissions identified by process SCC to each hour of the day, day of the week, and month.

[18] In order to simplify the implementation of the processed EI in a variety of forecast models and to keep its size manageable, we did not consider the more complex treatments available in detailed emissions processing systems such as the Sparse Matrix Operator Kernel Emissions (SMOKE) model system (http://www.baronams.com/products/smoke/). For example, processed emissions were available for each hour of an OSD, but emissions for specific days of the week or months were not compiled. The effect of temperature on emissions was not included in the processed inventory because of the necessary coupling between the emission data set and the meteorological models. Instead, NEI99 emissions prepared by the EPA and state air quality agencies using climatological average temperatures were included without modification. The detailed temporal and meteorological patterns in emissions are an additional modulation to the large year-to-year changes in power plant NO_x emissions, but these patterns have been ignored for the purposes of the model studies described.

[19] All emissions from biogenic vegetative sources, wildfires, and prescribed and managed burning were omitted from the processed inventory. The vegetative sources were already being treated in detail by the individual forecast models operating during NEAQS2K4 through the use of biogenic emission modules coupled to predicted variables such as temperature and sunlight. Natural and anthropogenic burning varies greatly from year to year both in the magnitude of emissions and their location, so that emissions derived for a previous year were not appropriate to summer 2004. Wildfire and anthropogenic burning emissions can be significant depending on the time and region studied. However, WP-3 and other aircraft observations and the FLEXPART model using satellite-derived fire products (http://niwot.al.noaa.gov:8088/icartt_analysis/) indicate that there was relatively little impact of fire emissions over the period of NEAQS2K4 and spatial domain considered in this study.

[20] The complete processed reference EI is publicly available. See http://ruc.fsl.noaa.gov/wrf/WG11/anthropogenic.htm for more details of the data set, and contact the first author for download instructions. A geographic information system (GIS) interface, the Emission Inventory Mapviewer, http://map.ngdc.noaa.gov/website/al/emissions, was developed to allow users to easily visualize the processed emissions along with various geographic data layers, download selected point source emissions, and quantify gridded emissions within any latitude-longitude box.

2.3. Power Plant Emission Updates

[21] Fifty-three U.S. power plants were selected for emission updates to account for controls implemented between 1999 and 2003 (Table 1). The choice of these plants was based on their 1999 NO_x and SO_2 emissions, the availability of observations of their emission plumes during field experiments in 1995, 1999, 2000, and 2004, and their locations relative to the study region of interest. Throughout the rest of this paper, these 53 power plants are referred to as the perturbation plants. Figure 1 shows the NEI99 annual NO_x and SO_2 emissions for all large point sources in the eastern United States and highlights the perturbation plants. The point sources in Figure 1 with the largest NO_x and SO_2 emissions are almost all coal-burning power plants. Nearly all the perturbation plants burn coal, with the exception of a few oil-burning units at Brayton Point, Canal, Salem Harbor, and Chalk Point and some or all units that burn natural gas at Chalk Point, Robinson, Tradinghouse, and Parish. The perturbation plants represent a quarter of 1999 U.S. total power plant NO_x emissions and a third of U.S. SO_2 power plant emissions. The perturbation plants account for 30% of NO_x and 35% of SO_2 emitted in 1999 by U.S. power plants within the domain shown in Figure 1 and for 18% of NO_x and 27% of SO_2 emitted by all U.S. point sources in this region. This selected list of 53 plants, while not exhaustive, is a representative sample of the power plant sources in the eastern United States.

[22] Updates to the NEI99 NO_x and SO_2 emissions of the perturbation power plants were made as follows. When the model simulations discussed here were carried out, the latest summer CEMS data available on the Clean Air Markets site (http://www.epa.gov/airmarkets/emissions) were for the third calendar quarter (July to September) of 2003. The mass of NO_x (as NO_2) or SO_2 emitted by a power generation unit (boiler plus any attached stacks) during a specified time period divided by the heat input to the boiler during the same period is defined as the emission rate, reported as pounds of NO_x or SO_2 emitted per million British Thermal Units (mmBTU) of heat input (Table 1). The emission rate normalizes the absolute emissions to remove differences in power generation activity over time and to isolate the changes due to the use of control technology on each unit. U.S. power generation activity, as measured by total boiler heat input, increased by about 6% between 1999 and 2003 (http://www.epa.gov/airmarkets/emissions), so changes in absolute emissions during this period also resulted primarily from implementation of pollution controls. For NO_x and SO_2 emissions from the perturbation plants, the ratio of the 2003 third quarter CEMS emission rate to the 1999 third quarter CEMS emission rate was calculated for each generation unit at each plant (Table 1). The NEI99 OSD NO_x and SO_2 emissions at each of the perturbation plants' units were then multiplied by the CEMS 2003/1999 emission rate ratios. The resulting inventory, hereafter referred to as the perturbation EI, had the same format as the processed reference EI based on the NEI99, except that the emission rates of the perturbation plants had been updated to their summer 2003 levels.

[23] Ideally all power plants in the NEI99 would have been updated to their 2003 emission rates using the full CEMS data set according to the above procedure. The difficulty in this approach stems from the differences in the identification of individual power generation units at a particular plant and the distribution of emissions across

Table 1. For Each of the 53 Perturbation Plants Described in the Text, the NEI 1999 Annual Mass Emissions and Average Hourly Molar Emissions on an Ozone Season Day, the CEMS Emission Rates for the First and Third Quarters of 1999 and 2003, the Ratio of the 2003 to 1999 Third Quarter CEMS Emission Rates, and the Difference Between the Reference and Perturbation EI OSD Average Hourly Molar Emissions

		1999 NEI,[a] kton/yr		1999 NEI,[b] kmol/hr		1999Q1 CEMS,[c] lb/mmBTU		1999Q3 CEMS,[c] lb/mmBTU		2003Q1 CEMS,[c] lb/mmBTU		2003Q3 CEMS,[c] lb/mmBTU		2003/1999 Q3 CEMS[d]		Ref – Pert EI,[e] kmol/hr	
Plant	State	NO_x	SO_2	NO_x	SO_2	NO_x	SO_2	NO_x	SO_2	NO_x	SO_2	NO_x	SO_2	NO_x	SO_2	NO_x	SO_2
Amos	WV	55.6	108.6	116.5	165.3	0.634	1.260	0.603	1.234	0.676	1.350	0.317	1.298	0.524	1.052	55.4	−8.6
Baldwin	IL	55.0	245.2	138.0	438.2	1.106	5.114	1.088	5.145	0.406	0.401	0.267	0.404	0.245	0.078	104.1	403.8
Big Brown	TX	12.9	83.8	32.7	152.4	0.350	2.152	0.356	2.278	0.154	1.798	0.142	1.815	0.398	0.797	19.7	31.0
Bowen	GA	41.7	138.9	105.7	253.2	0.426	1.423	0.422	1.431	0.417	1.547	0.055	1.563	0.129	1.092	92.0	−23.4
Brandon Shores	MD	22.5	54.5	49.9	87.4	0.518	1.086	0.334	1.073	0.507	1.047	0.114	1.019	0.342	0.949	32.9	4.4
Brayton Point	MA	14.4	48.9	30.8	74.2	0.347	1.140	0.314	1.040	0.344	1.095	0.297	1.006	0.946	0.967	1.7	2.4
Brunner Island	PA	12.5	71.2	27.1	109.7	0.396	2.214	0.292	2.032	0.392	1.857	0.296	1.897	1.015	0.933	−0.4	7.3
Canal	MA	7.9	27.9	18.5	46.9	0.252	0.868	0.230	0.883	0.279	1.064	0.134	1.000	0.586	1.132	7.7	−6.2
Cardinal	OH	33.2	115.0	83.7	193.6	0.811	2.578	0.718	2.328	0.596	1.949	0.188	1.702	0.261	0.731	61.9	52.1
Chalk Point	MD	25.7	57.6	64.2	102.4	0.518	1.543	0.544	1.174	0.412	1.429	0.343	1.629	0.630	1.387	23.7	−39.6
Chesapeake	VA	10.7	35.3	24.8	58.8	0.525	1.534	0.428	1.570	0.463	1.412	0.180	1.490	0.420	0.949	14.4	3.0
Cheswick	PA	5.2	41.6	11.0	62.8	0.383	2.549	0.252	2.557	0.396	2.527	0.045	2.516	0.179	0.984	9.0	1.0
Conemaugh	PA	20.8	7.9	47.7	13.1	0.394	0.125	0.262	0.129	0.362	0.107	0.315	0.128	1.203	0.988	−9.7	0.2
Conesville	OH	23.8	144.9	59.6	257.9	0.481	2.785	0.465	3.254	0.527	2.382	0.510	2.568	1.097	0.789	−5.8	54.4
Cumberland	TN	82.7	15.9	199.3	26.6	1.072	0.176	0.953	0.191	0.554	0.179	0.381	0.247	0.400	1.291	119.6	−7.7
Eastlake	OH	16.9	115.6	46.8	223.4	0.483	4.008	0.625	4.372	0.656	1.985	0.636	2.225	1.017	0.509	−0.8	109.7
Ft Martin	WV	30.4	99.1	72.6	169.4	0.758	2.656	0.806	2.527	0.304	2.746	0.312	2.677	0.386	1.059	44.6	−10.1
Gallatin	TN	13.0	84.8	29.1	137.0	0.376	2.660	0.323	2.035	0.326	0.863	0.299	0.761	0.924	0.374	2.2	85.8
Gavin	OH	51.9	15.2	125.8	25.7	0.728	0.141	0.621	0.210	0.600	0.343	0.289	0.363	0.465	1.725	67.3	−18.6
Gibson	IN	49.4	158.9	114.9	259.8	0.453	1.642	0.451	1.322	0.484	1.732	0.275	1.172	0.610	0.887	44.8	29.3
Gorsuch	OH	5.7	80.3	13.6	136.3	0.721	8.875	0.578	9.117	0.342	3.559	0.370	3.718	0.640	0.408	4.9	80.7
Harrison	WV	34.7	6.8	80.1	11.3	0.467	0.112	0.487	0.084	0.484	0.150	0.115	0.146	0.236	1.740	61.2	−8.4
Hatfields Ferry	PA	20.1	141.9	42.9	217.9	0.445	3.315	0.428	3.369	0.469	2.051	0.287	3.367	0.670	0.999	14.1	0.1
Homer City	PA	26.6	163.4	56.1	250.0	0.451	2.665	0.377	2.579	0.469	2.051	0.107	2.234	0.284	0.866	40.2	33.4
Johnsonville	TN	20.4	119.8	49.9	210.9	0.478	2.766	0.479	2.960	0.530	2.465	0.516	2.269	1.076	0.767	−3.8	49.2
Keystone	PA	20.4	162.3	44.1	251.8	0.376	2.637	0.301	2.780	0.336	2.728	0.042	2.705	0.141	0.973	37.9	6.7
Kyger Creek	OH	30.3	135.6	66.5	213.6	0.949	3.315	0.751	4.190	0.806	2.391	0.377	2.035	0.502	0.486	33.1	109.9
Limestone	TX	24.9	32.9	57.8	54.9	0.426	0.550	0.428	0.560	0.236	0.545	0.210	0.527	0.490	0.940	29.4	3.3
Mansfield	PA	23.4	27.1	51.6	43.0	0.422	0.399	0.306	0.413	0.444	0.409	0.191	0.435	0.624	1.053	19.4	−2.3
Martin Lake	TX	28.4	111.6	66.8	189.0	0.343	1.137	0.265	1.143	0.184	0.770	0.160	0.921	0.604	0.806	26.5	36.7
Mercer	NJ	12.8	12.8	27.9	20.7	1.001	0.863	0.630	0.815	0.853	0.979	0.612	0.947	0.971	1.162	0.8	−3.4
Merrimack	NH	7.9	34.8	17.5	55.7	0.846	2.216	0.376	2.396	0.281	1.743	0.154	1.638	0.409	0.684	10.3	17.6
Monroe	MI	50.8	111.3	120.3	188.7	0.566	1.295	0.574	1.291	0.540	1.290	0.312	1.360	0.544	1.053	54.9	−10.1
Monticello	TX	20.5	100.1	48.6	171.4	0.277	1.320	0.260	1.268	0.203	1.107	0.167	1.083	0.641	0.854	17.5	25.0
Montour	PA	15.9	113.7	36.8	189.1	0.447	2.850	0.315	2.838	0.434	2.717	0.041	2.641	0.131	0.930	32.0	13.2
Morgantown	MD	22.1	75.5	52.6	128.8	0.627	2.423	0.626	2.076	0.526	2.151	0.368	2.306	0.588	1.111	21.6	−14.3
Mountaineer	WV	20.5	44.7	43.9	68.9	0.497	1.105	0.495	1.098	0.608	1.074	0.056	1.020	0.113	0.929	39.0	4.9
Muskingum River	OH	21.4	100.6	54.1	190.6	0.795	3.569	0.677	3.272	0.767	3.677	0.622	3.845	0.918	1.175	4.5	−33.4
New Madrid	MO	52.2	16.4	141.5	31.8	1.383	0.421	1.241	0.406	1.324	0.392	0.811	0.387	0.654	0.954	49.0	1.5
Paradise	KY	104.4	181.1	255.9	309.2	1.405	1.951	1.380	2.451	0.787	1.275	0.257	1.577	0.187	0.643	208.2	110.3
Parish	TX	33.4	67.6	85.8	119.9	0.323	0.649	0.264	0.465	0.146	0.611	0.086	0.626	0.326	1.346	57.9	−41.5
Pleasants	WV	14.1	44.1	33.4	75.1	0.374	1.111	0.325	1.112	0.397	1.128	0.078	1.146	0.241	1.031	25.3	−2.3
Robinson	TX	8.6	0.0	26.9	0.1	0.170	0.001	0.203	0.001			0.163	0.001	0.803	1.013	5.3	0.0
Salem Harbor	MA	6.0	23.7	11.1	30.5	0.283	1.328	0.294	1.057	0.296	0.938	0.232	0.814	0.791	0.770	2.3	7.0
Sammis	OH	58.7	150.8	141.2	261.3	0.771	2.040	0.736	1.958	0.509	2.058	0.486	1.992	0.660	1.018	48.0	−4.6
Sporn	WV	20.1	67.1	42.7	103.8	0.784	2.563	0.664	2.415	0.509	1.709	0.482	1.704	0.726	0.706	11.7	30.5
Stuart	OH	49.7	102.0	109.3	160.9	0.756	1.447	0.647	1.411	0.626	1.610	0.639	1.684	0.988	1.194	1.3	−31.2
Thomas Hill	MO	31.3	21.1	69.9	34.2	0.651	0.415	0.613	0.418	0.469	0.411	0.429	0.421	0.701	1.007	20.9	−0.3
Tradinghouse	TX	15.15	0.02	39.6	0.0	0.444	0.001	0.497	0.001	0.235	0.037	0.227	0.002	0.457	2.757	21.5	−0.1
Wansley	GA	19.6	79.9	49.6	145.0	0.411	1.620	0.399	1.700	0.316	1.572	0.051	1.560	0.129	0.918	43.2	11.9
Welsh	TX	22.9	38.0	53.0	62.8	0.355	0.683	0.380	0.598	0.283	0.559	0.233	0.589	0.611	0.985	20.6	0.9
Willow Island	WV	9.3	17.3	21.4	29.0	1.180	1.912	1.031	2.039	0.851	2.006	0.851	1.933	0.826	0.948	3.7	1.5
Yates	GA	9.9	35.2	28.0	70.4	0.386	1.307	0.300	1.080	0.410	1.628	0.274	1.220	0.911	1.129	2.5	−9.1

[a]NEI99 annual mass emissions in tons per year.
[b]NEI99 ozone season day (OSD) average hourly molar emissions.
[c]CEMS emission rates for the first and third quarters (Q1 and Q3) of 1999 and 2003.
[d]Ratio of the CEMS third quarter 2003 to third quarter 1999 emission rates.
[e]Difference between the perturbation and reference EI OSD average hourly molar emissions = (NEI99 OSD)*(1 − (2003Q3 CEMS/1999Q3 CEMS)).

these units. The CEMS data are reported for individual boilers at a specific plant identified according to the U.S. Department of Energy's ORIS plant and boiler codes. In the NEI, a given boiler's emissions can be allocated between multiple stacks and processes. The cross referencing of the CEMS and NEI identifiers for a particular boiler-stack-process is not always straightforward, and in many cases this allocation must be carried out manually. Given the amount of time involved in making accurate allocations of the CEMS data to NEI power generation units, the update

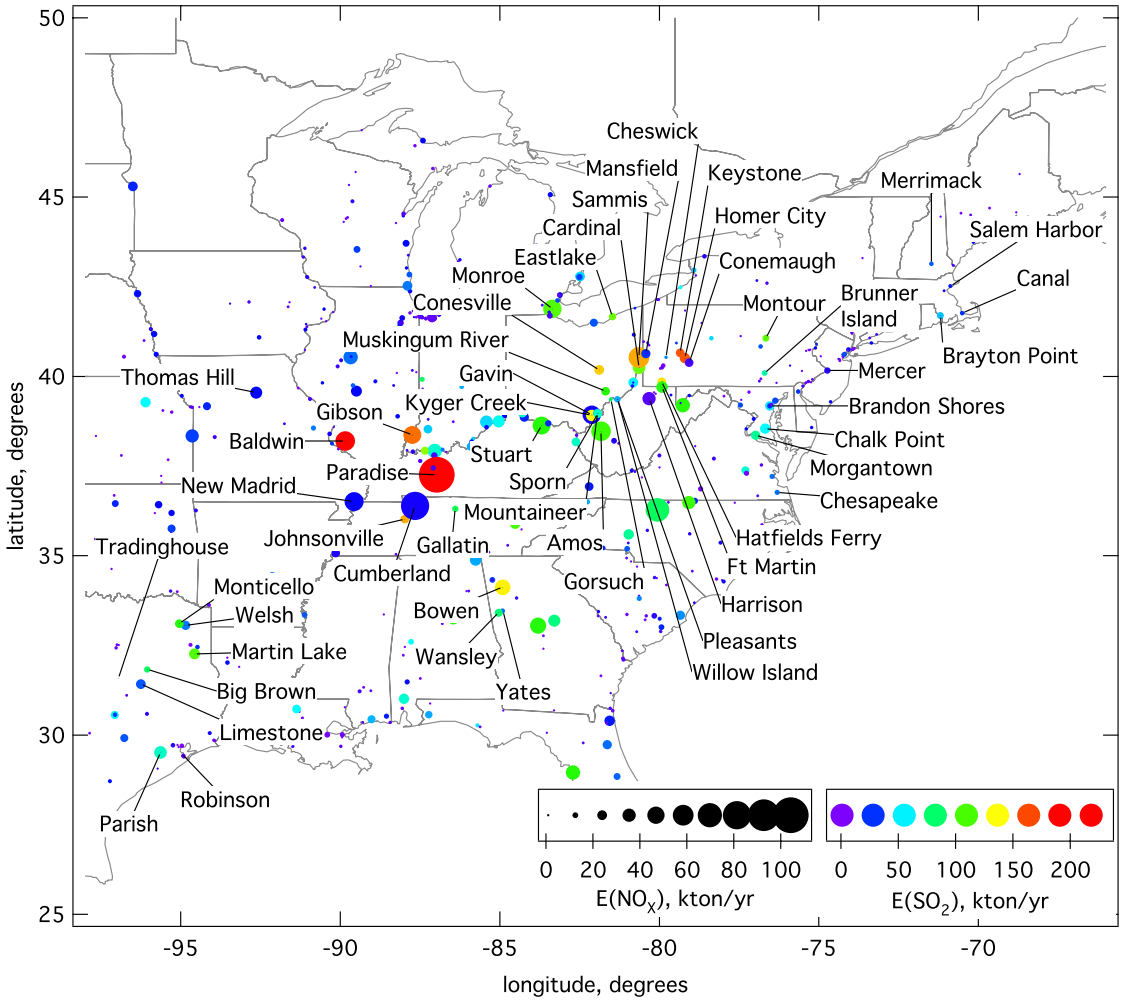

Figure 1. Point emission sources in the eastern United States. The EPA NEI99 annual mass emissions (in kton/yr) for NO_x are denoted by the size of the circles, and those for SO_2 are given by the symbol color. Only point sources with emissions greater than 1000 tons per year of either NO_x (as NO_2) or SO_2 are shown. The names and locations of the 53 power plants whose emissions were updated using 2003 CEMS data (see text) are indicated. Symbols overlap for a few perturbation plants in close proximity to each other. Highest emitting U.S. point sources in 1999: NO_x = 104 kton/yr (Paradise), SO_2 = 245 kton/yr (Baldwin).

process was carried out for only the limited number of plants discussed above.

2.4. WRF-Chem Model

[24] The impact of these EI updates is investigated using the Weather Research and Forecasting model with online Chemistry (WRF-Chem). WRF-Chem is based upon version 2 of the nonhydrostatic WRF community model developed at the National Center for Atmospheric Research (NCAR) (http://www.mmm.ucar.edu/wrf/users). Details of WRF-Chem can be found in *Grell et al.* [2005] and at http://ruc.fsl.noaa.gov/wrf/WG11/. This model is an extension of the earlier MM5/Chem regional-scale chemical transport model [*Grell et al.*, 2000] to the WRF architecture. Real-time WRF-Chem forecasts can be found at http://www-frd.fsl.noaa.gov/aq/wrf/. This numerical model system is "online" in the sense that all processes affecting the gas phase and aerosol species are calculated in lock step with the meteorological dynamics. Meteorological initial conditions are taken from the Rapid Update Cycle (RUC) model analysis fields generated at NOAA Earth System Research Laboratory/Global Systems Division, and lateral boundary conditions are derived from the NOAA National Centers for Environmental Prediction (NCEP) Eta model forecast. Gas-phase chemistry is based upon the Regional Acid Deposition Model version 2 (RADM2) [*Stockwell et al.*, 1990] with updates to the original mechanism [*Stockwell et al.*, 1997]. Biogenic emissions are calculated at each time step using the BEIS3.11 algorithm (http://www.epa.gov/asmdnerl/biogen.html). The WRF-Chem retrospective simulations discussed in this work are 36-hour forecasts starting at 0000 UTC each day. The horizontal domain of 134 × 110 grid points has a grid spacing of 27 km and is centered at 86.3°W and 38.0°N. The spacing of the model's 35 vertical levels is about 16 m near the surface and increases to about 1.5 km at the top of the domain (at ~18 km). Other WRF-Chem configuration options used in these simulations are given in Table 2.

Table 2. WRF-Chem Model Configuration Used for This Study[a]

Parameter	Option Used
Advection scheme	fifth order horizontal/third order vertical
Microphysics	NCEP 3-class simple ice
Longwave radiation	RRTM
Shortwave radiation	Dudhia
Surface layer	Monin-Obukhov (Janjic Eta)
Land surface model	RUC-LSM
Boundary layer scheme	M-Y-J 2.5 TKE
Cumulus parameterization	Grell-Devenyi
Photolysis scheme	TUV [*Madronich*, 1987]
Dry deposition	flux-resistance method [*Wesley*, 1989; *Erisman et al.*, 1994; *Slinn and Slinn*, 1980]
Chemistry option	RADM2
Aerosol option	MADE/SORGAM

[a]Details about the model configuration options and references for the physical parameterizations used in each module are given by *Grell et al.* [2005] and at http://ruc.fsl.noaa.gov/wrf/WG11/.

[25] Two WRF-Chem retrospective cases are examined. The reference case uses the processed reference EI based on the NEI99. The perturbation case uses the perturbation EI, in which the NEI99 NO_x and SO_2 emissions for the 53 perturbation plants were updated using the ratio of the 2003/1999 CEMS emission rate data. In all other respects the reference and perturbation cases are identical, including initial meteorological fields and chemical concentrations, as well as emissions of all other sources besides the perturbation plants. Feedbacks between gas and aerosol phase chemical fields and the meteorological variables have been turned off in these simulations, so that observed changes in chemical variables between the reference and perturbation cases are solely due to changes in the emissions of the selected power plants.

3. Results

3.1. Changes in Power Plant Emissions

[26] Summertime NO_x emission rates decreased between 1999 and 2003 at most of the 53 perturbation plants (Table 1). Figure 2 shows the 1999 and 2003 third quarter CEMS NO_x and SO_2 emission rates for these plants in order of decreasing 1999 NO_x emission rate. For nearly two thirds of the plants, the decreases in the 2003 summer NO_x emission rates relative to summer 1999 are outside the estimated uncertainty limits on the CEMS data (see next paragraph). Nearly half of the plants show NO_x emission rate reductions of 50% or more between 1999 and 2003, and several reduced NO_x emission rates by between 80 and 90% over this period. The overall NO_x emission rate of the perturbation plants decreased 49%, from 0.516 to 0.265 lb (of NO_2) $mmBTU^{-1}$.

[27] Systematic studies of uncertainty limits on CEMS data have not been presented in the peer-reviewed literature. A review of stationary source emissions [*Placet et al.*, 2000] cites a conference proceedings report that NO_x and SO_x CEMS data achieve an accuracy of within 10%. Extensive analysis of aircraft measurements of power plant plumes from field missions over the last 6 years (T. Fortin et al., Airborne evaluations of power plant emissions derived from CEMS data, manuscript in preparation, 2006), using methods described by *Ryerson et al.* [1998, 2001, 2003], indicates that CEMS data for the plants studied have a total 2σ uncertainty of ±24%. We use the more conservative uncertainty limits in the comparisons of CEMS data presented here.

[28] In contrast to NO_x, summertime SO_2 emission rates changed little between 1999 and 2003 at most plants (Figure 2 and Table 1). The perturbation plants' total SO_2 emission rate decreased from 1.52 to 1.32 lb $mmBTU^{-1}$, a change of 13%. Large decreases in SO_2 emission rates are seen at a few plants,

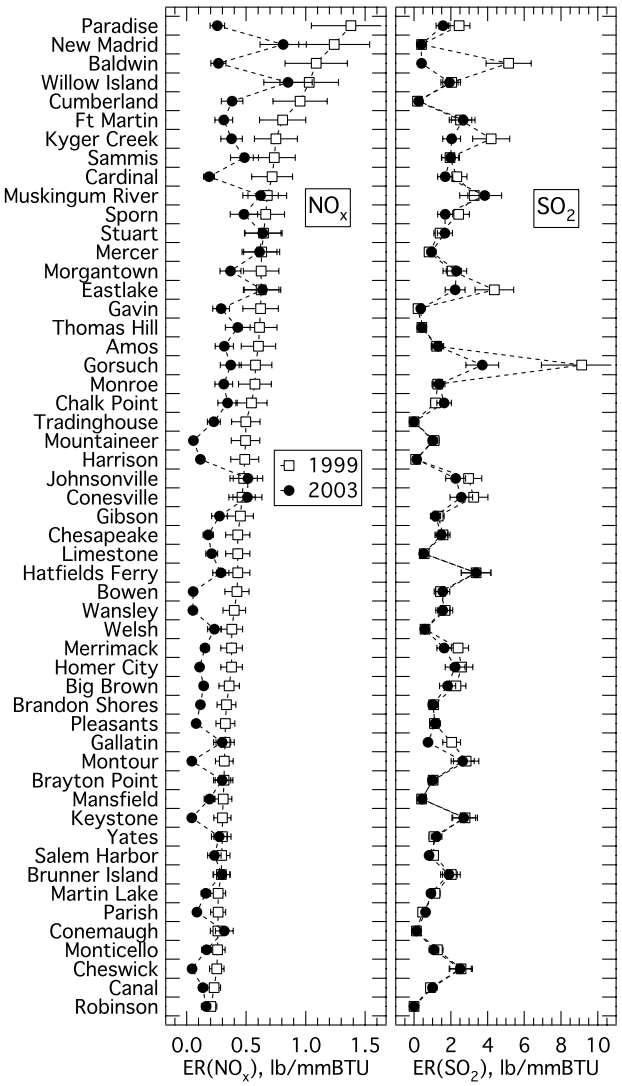

Figure 2. Third quarterly (July to September) average CEMS emission rates (ER) for (left) NO_x and (right) SO_2 in 1999 (open squares) and 2003 (solid circles) at the 53 perturbation plants, in order of decreasing 1999 NO_x emission rate. Average emission rates at a particular plant are the ratio of total quarterly mass emissions (in pounds) divided by total quarterly heat input (in million British Thermal Units). Plant totals are a sum over individual power generation units. Not all units at a given plant implemented pollution controls between 1999 and 2003, so individual units within the same plant may not have the same magnitude or direction of change in emissions during this period. Bars on CEMS data are ±24% 2σ (2 standard deviations) uncertainty estimates discussed in the text.

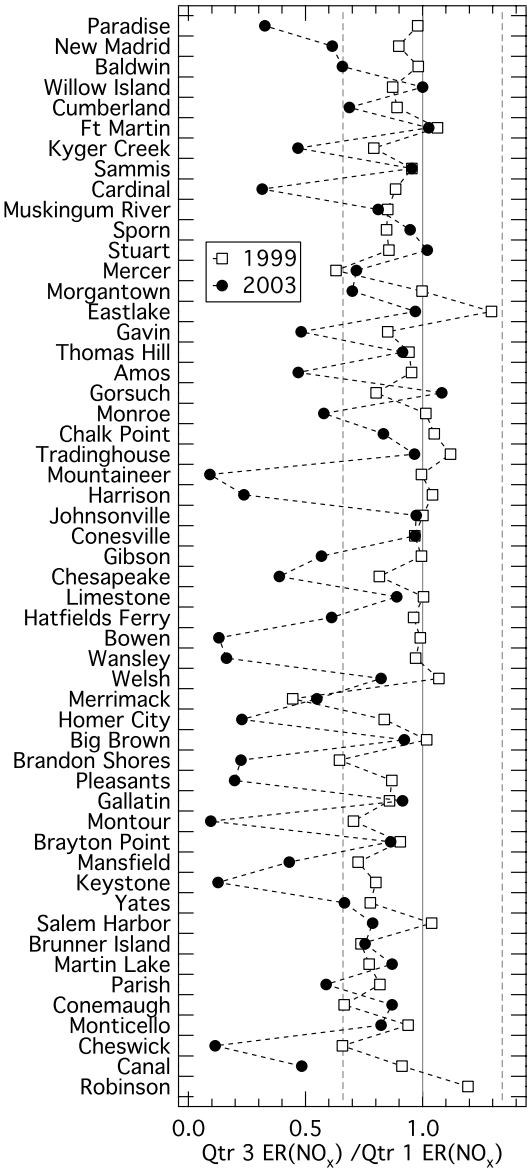

Figure 3. Ratio of the CEMS third to first quarterly average NO_x emission rates (ER) for 1999 (open squares) and 2003 (solid circles) at the 53 perturbation plants. Solid gray line is a ratio of 1, and dotted gray lines are ±34% (2σ) combined uncertainty limits on the unit ratio (see text).

particularly Baldwin (Illinois) and Gorsuch (Ohio). Significant SO_2 reductions had already occurred throughout the United States between 1990 and 1995 in response to the Acid Rain Program [*U.S. EPA*, 2003].

[29] The CEMS data (Table 1) reveal significant differences in the seasonal cycle of NO_x emission rates between 1999 and 2003 at the perturbation plants (there are essentially no seasonal differences in the SO_2 emission rates in either year). Figure 3 compares the 1999 and 2003 ratios of CEMS third quarter (summer) to first quarter (winter) NO_x emission rates. NO_x emission rates in summer 1999 were lower than those in winter 1999 at many plants, although the differences are within the combined CEMS uncertainties for all but a couple of plants. The average 1999 summer to winter NO_x emission rate ratio for the perturbation plants is 0.90, well within the uncertainties in the CEMS data. The 2003 NO_x emission rates show a much stronger seasonal cycle than those in 1999. Summer 2003 NO_x emission rates were generally much lower than those in winter 2003, with an average perturbation plant summer to winter ratio of 0.63. For reference (Table 1), 1999 and 2003 winter NO_x emission rates were similar for nearly all plants except those with the highest NO_x emissions. The effect of NO_x emission control technologies applied only during the ozone season (such as SCR and SNCR) is clearly apparent in the 2003 CEMS data.

3.2. CEMS Validation Using Aircraft Observations

[30] The 2003 and 2004 third quarter CEMS molar emission ratios of SO_2 to NO_x, E(SO_2)/E(NO_x), for 19 plants are compared to the SO_2/NO_{yi} ratios measured on board the NOAA WP-3 aircraft (Figure 4). Emissions from these plants were sampled by the WP-3 during a total of 27 plume transects from 4 flights. All aircraft data were measured during periods of steady horizontal flow at downwind distances of between 2 km and 70 km, corresponding to plume travel times of roughly a few minutes to 2.5 hours depending on wind speed. Most of the plumes were sampled within 25 km of their point of emission, which translates to 40–85 min maximum elapsed travel time since emission assuming constant wind speed. With the exception of two plumes intercepted at roughly 1300 and 2300 m, all plume transects were made between 500 and 1200 m

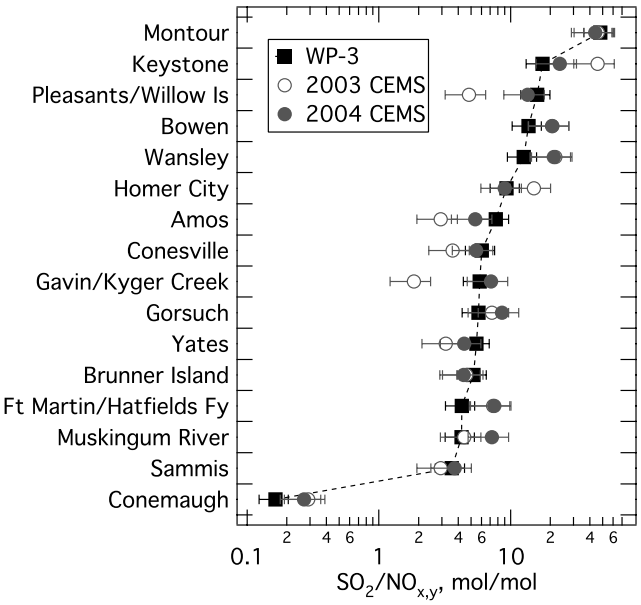

Figure 4. Comparison of 2004 NOAA WP-3 measured SO_2/NO_{yi} molar ratios (black squares) to third quarter CEMS E(SO_2)/E(NO_x) molar emission ratios from 2003 (gray open circles) and 2004 (gray solid circles) at 19 perturbation plants. Data are arranged in order of decreasing WP-3 SO_2/NO_{yi} ratio. Bars on CEMS data are ±34% (2σ) combined uncertainties. Bars on WP-3 measurements are the ±25% (2σ) uncertainties in the slopes of the fits to the SO_2 to NO_{yi} correlations in each plume transect. See text for further explanation.

altitude above ground level. In a few cases the plumes from 2 nearby plants converged to an extent that the individual plant plumes could not be distinguished in the WP-3 measurements, so a composite CEMS SO_2/NO_x emission ratio for the two plants was compared instead.

[31] Plume SO_2/NO_{yi} was derived from the slope of a least squares fit to the observed SO_2 versus NO_{yi} for a flight segment including the plume transect as well as background air just outside the plume [*Ryerson et al.*, 1998]. The correlation coefficient, r, for these fits was 0.9 or larger. The uncertainty in the observed slope of the WP-3 SO_2 versus NO_{yi} correlations was estimated to be ±25% (2σ).

[32] For each of the plants or plant composites shown in Figure 4, the WP-3 observations and 2004 CEMS data agreed to within the combined uncertainties of ±40%. A linear fit to the correlation plot of 2004 CEMS E(SO_2)/E(NO_x) versus WP-3 SO_2/NO_{yi} for the plants shown in Figure 4 has a slope of 0.93 (r = 0.95). WP-3 SO_2/NO_{yi} emission ratios ranged from 0.16 mol/mol to 50 mol/mol, with most plants emitting between 4 and 20 moles of SO_2 for every mole of NO_x emitted. A similar level of agreement between 1999 CEMS data and WP-3 observations of SO_2 and NO_y was seen in other studies [*Ryerson et al.*, 1998, 2001, 2003].

[33] The 2004 third quarter CEMS data are used here since they should represent the actual emission ratios observed during the WP-3 flights. However, 2003 and 2004 third quarter CEMS E(SO_2)/E(NO_x) were similar for nearly all of these plants (Figure 4). In only 2 cases did the 2003 and 2004 CEMS emission ratios differ significantly, and in each case the 2004 CEMS E(SO_2)/E(NO_x) ratios were higher than those for 2003, as would be expected if further E(NO_x) reductions took place between 2003 and 2004.

[34] These comparisons assume that, prior to the WP-3 measurement, all emitted SO_2 was conserved and that emitted NO_x was either conserved or oxidized to other NO_y species that were conserved. This assumption could not be strictly confirmed experimentally in NEAQS2K4 because plumes were not generally sampled at multiple downwind points. However, our previous experience with sampling at the relatively short downwind distances and plume travel times employed in NEAQS2K4 indicates that SO_2 and NO_y are conserved to within the measurement uncertainties [*Ryerson et al.*, 1998, 2001, 2003]. The lifetime of SO_2 with respect to gas phase OH reaction is relatively long, on the order of 1–2 days. Cloud chemistry of SO_2 seems unlikely given the relatively clear skies between the WP-3 and the sampled plants. Measured NO_y is still about 70% unoxidized NO_x on average at the time of sampling by the WP-3. Deposition and other physical losses of NO and NO_2 are relatively slow. The other principal component of NO_y in these plumes is HNO_3. Its loss rate in similar previous plume measurements is highly variable, ranging from negligible within the measurement uncertainties to 0.65 hr^{-1} [*Ryerson et al.*, 1998, 2001, 2003; *Neuman et al.*, 2004]. Assuming the most rapid measured loss rate of HNO_3 from *Neuman et al.* [2004], the plume travel time noted above, and that the oxidized portion of NO_y is completely HNO_3, we calculate that NO_y could be at most 25% less than the emitted values, which is comparable to the uncertainty in the measurements themselves. Finally, we note that no consistent bias is seen between the WP-3 and CEMS emission ratios.

3.3. Power Plant EI Update

[35] A consistency check was performed on the 1999 power plant emissions within the NEI using CEMS data for that year. As expected, NEI99 ozone season NO_x and SO_2 average hourly molar emissions from the perturbation plants agreed with the CEMS 1999 third quarter data, since CEMS data were used to construct the NEI99. The NEI99 power plant emissions, like the CEMS 1999 data, showed the lack of a significant seasonal cycle, with essentially no difference between the annual and ozone season day average hourly emissions of NO_x or SO_2.

[36] The agreement between the 1999 CEMS and NEI99 data sets for the perturbation plants and the correspondence between the 1999 and 2004 summer CEMS data and WP-3 observations for many of these plants validated the use of the 2003 CEMS data to update the NEI99 emissions of the perturbation plants. As described in the Methods section, NEI99 OSD NO_x and SO_2 emissions were scaled by the ratio of the 2003 to 1999 third quarter CEMS emission rates (Table 1). The most appropriate updated inventory would have used 2004 rather than 2003 CEMS data, but the 2004 third quarter data were not available at the time that the inventory was prepared and the model simulations were carried out. Given the difficulties and time involved in correctly allocating the CEMS data to the NEI point sources and the relatively small differences between 2003 and 2004 emissions at most plants (Figure 4), the updates discussed here rely on the 2003 CEMS data set to demonstrate the methodology.

[37] Figure 5 and Table 1 show the differences in the average hourly molar NO_x and SO_2 emissions between the reference and perturbation EIs at the 53 perturbation power plants. The 8 plants with the largest E(NO_x) decreases were Paradise (Kentucky), Cumberland (Tennessee), Baldwin (Illinois), Bowen (Georgia), Gavin (Ohio), Cardinal (Ohio), Harrison (West Virginia), and Parish (Texas). The largest E(SO_2) decrease was at Baldwin, with more modest reductions at Paradise, Kyger Creek (Ohio), Eastlake (Ohio), Gallatin (Tennessee), and Gorsuch (Ohio). Because of the widespread decreases in power plant NO_x emission rates between 1999 and 2003 and their direct impact on O_3, the remainder of the paper will focus on the changes in NO_x emissions and their effects on O_3.

3.4. Model Reference Scenario

[38] WRF-Chem retrospective simulations were carried out for 1–21 July 2004. The results discussed throughout the rest of the paper are from simulations starting at 0000 UTC on 21 July 2004. Model output for 21 July 2004 at 2000 UTC (1500 Eastern Standard Time) is averaged over the first 12 vertical grid levels, or roughly 0 to 1 km above ground level. The calculated mixing ratios and their changes with respect to emission perturbations are similar at each model level up to about 1 km, roughly the height of the simulated mixed layer at its highest diurnal extent. We focus on the afternoon of 21 July 2004 because more of the perturbation plants were under clear skies than on other days in the 3-week period studied, resulting in larger O_3 impacts from emission changes. However, the

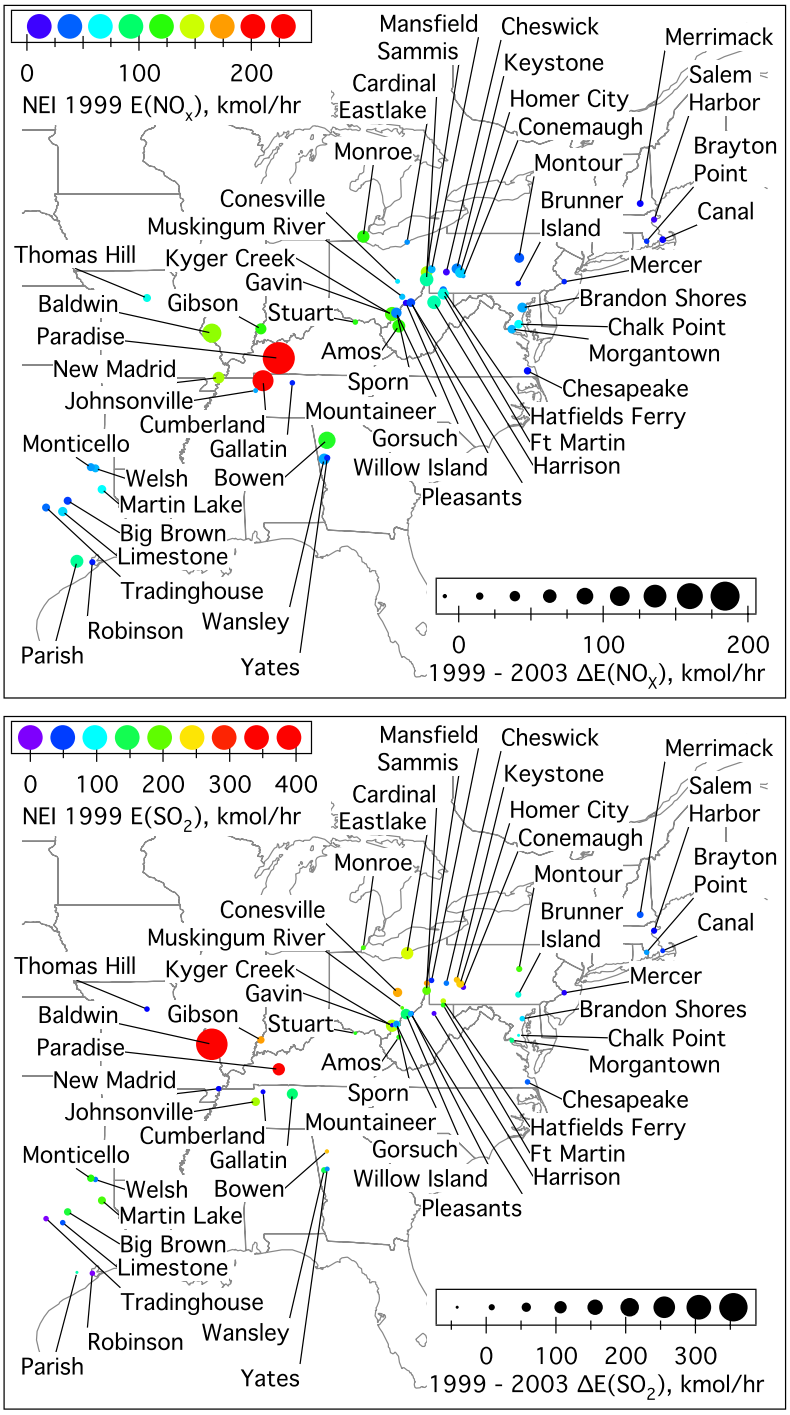

Figure 5. (top) NO_x and (bottom) SO_2 NEI99 ozone season average hourly molar reference emissions and the difference between the reference and 2003 perturbation inventories for the 53 perturbation plants, in kmol/hr. The color of each plant's symbol represents its 1999 reference emissions, and the size of the symbol indicates the difference in the emissions between the reference and perturbation EIs. Symbols overlap for a few perturbation plants in close proximity to each other. Maximum values: Reference E(NO_x) = 256 kmol/hr, Reference - Perturbation $\Delta E(NO_x)$ = 208 kmol/hr (Paradise); Reference E(SO_2) = 438 kmol/hr, Reference - Perturbation $\Delta E(SO_2)$ = 404 kmol/hr (Baldwin).

general picture presented by the 21 July model results is repeated on other days throughout the simulation period.

[39] Observed surface temperatures across the northern portion of the eastern United States were below the seasonal average for most of summer 2004 and particularly during NEAQS2K4. Both warm and cold fronts swept through this region of the country with an unusually high frequency. As a result there were few opportunities for pollution buildup

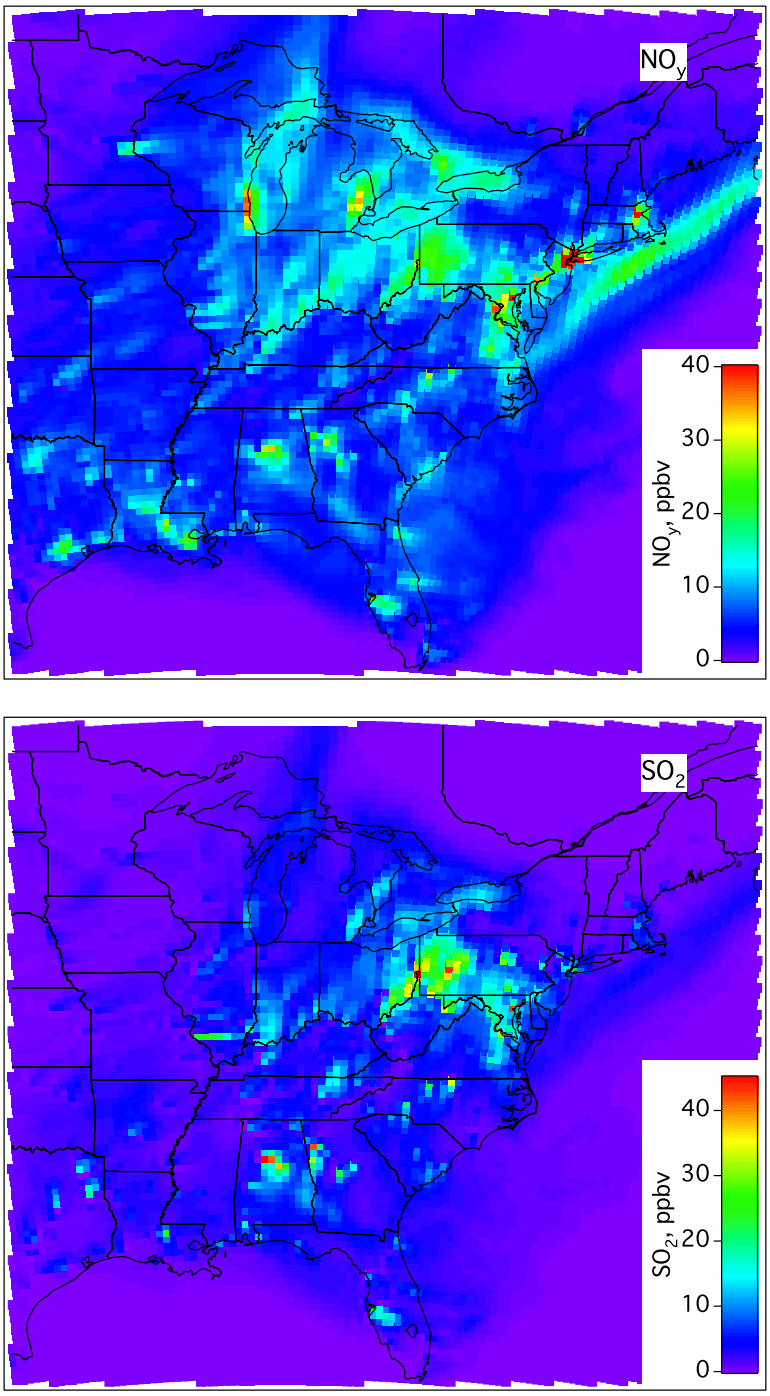

Figure 6. WRF-Chem reference emission inventory case (top) NO_y and (bottom) SO_2 mixing ratios (in ppbv) averaged over the lowest 12 altitude layers (approximately 0–1 km above ground level) at 2000 UTC on 21 July 2004. NO_y color scale saturates at the high end for better contrast. Maximum mixing ratios: NO_y = 94.4 ppbv, SO_2 = 46.1 ppbv.

during multiday stagnation events. The afternoon of 21 July was somewhat warmer and sunnier across the eastern United States than the previous few days as high pressure dominated much of the region. A low-pressure system traveling southeast through Canada was preceded by westerly to southerly flow over the northern half of the eastern United States, while relatively stagnant conditions behind a slow-moving cold front over the mid-Atlantic persisted across the southeastern United States.

[40] Figure 6 shows the simulated NO_y and SO_2 average mixing ratios between 0 and 1 km on the afternoon of 21 July for the reference emission case. NO_y maxima are widely distributed throughout the eastern United States, reflecting NO_x emissions from power plants, other industrial point sources, motor vehicles, and urban sources. SO_2 peaks are more localized, since they originate primarily from emissions of coal-fired power plants in the eastern United States. The colocation of SO_2 and NO_y plumes highlights the power

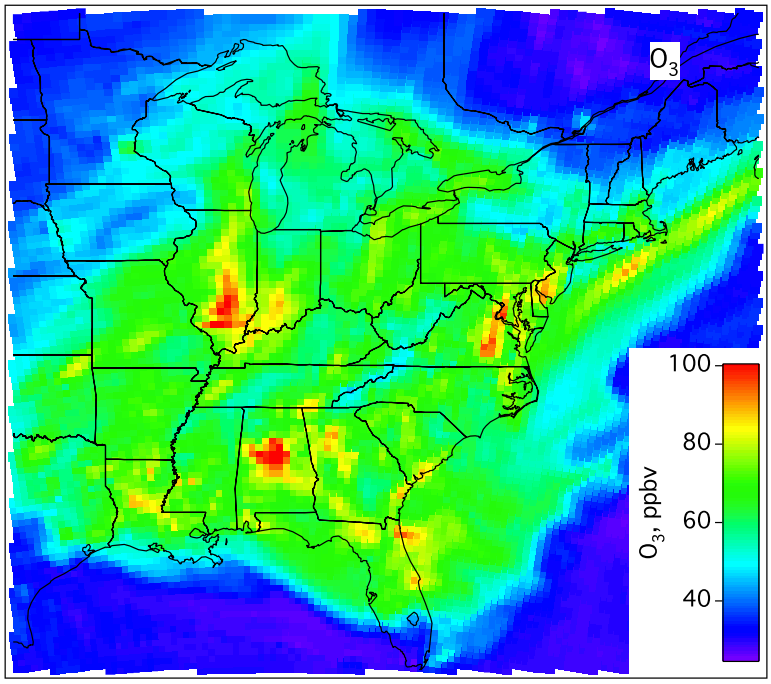

Figure 7. WRF-Chem reference emission inventory case O_3 mixing ratios (in ppbv) averaged over the lowest 1 km of the simulation domain at 2000 UTC on 21 July 2004.

plants. An extended plume of NO_y with little corresponding SO_2 to the east of the Atlantic coast urban areas is mostly pollution transported from these urban areas over the previous 24 hours.

[41] Simulated O_3 on the afternoon of 21 July reflects some of the NO_x emission pattern (Figure 7). Power plant NO_x emissions are at least partly responsible for local O_3 maxima in Illinois, Indiana, Ohio, Pennsylvania, Alabama, Georgia, and along the mid-Atlantic coast. High O_3 concentrations in the plume off the East Coast result predominantly from urban emissions. The extent of O_3 production in these plumes reflects not only E(NO_x) but also VOC emissions, particularly biogenic emissions of isoprene, and solar shortwave flux during transport. Elevated concentrations of O_3 are distributed more widely than high NO_y values, because of the time lag in photochemical production of O_3 after NO_x emission and transport and ozone's longer lifetime.

[42] Because of the relatively cool temperatures and frequent frontal disturbances in the summer of 2004, simulated O_3 levels in the northeastern United States are lower than would be expected on the basis of climatological averages. Because of relatively clear skies during the morning of 21 July and several days' worth of gradual warming, afternoon O_3 levels across the eastern United States on 21 July were on average a few ppbv higher than in previous days. Comparisons of WRF-Chem O_3 simulations to observations by a network of surface monitors in the northeastern United States [*McKeen et al.*, 2005] indicate that the model is capable of reproducing some of the spatial and temporal variability of the observations. *McKeen et al.* [2005] demonstrated that the ozone forecast reliability of version 1 of WRF-Chem (which used 1996 EPA emissions) was typical of the seven air quality forecast models compared during NEAQS2K4, with WRF-Chem median peak 1-hour and 8-hour average O_3 values 15 ppbv higher than observations. In the current WRF-Chem version 2 simulations using the NEI 1999, the model exhibited a median bias of only a few ppbv compared with NEAQS2K4 boundary layer WP-3 O_3 observations across a region similar to that examined by *McKeen et al.* [2005]. The model's bias in simulating O_3 mixing ratios is less important in the current study than its correct response to changes in emissions, which, as we show in the rest of the paper, is consistent with previous model and observational evidence.

3.5. Impact of Decreased NO_x Emissions on O_3

[43] In this section, NO_x and NO_y are used interchangeably when discussing the impact of E(NO_x) reductions on O_3. Emitted NO_x is converted to less reactive NO_y compounds in competition with O_3 photochemical production, through radical termination reactions ($NO_2 + OH \rightarrow HNO_3$) and conversion to reservoir species such as organic nitrates. Because NO_y has a longer lifetime than NO_x, it is a more conservative tracer of emitted NO_x than NO_x itself. Changes in NO_x and NO_y between the perturbation and reference EI cases result only from changes in power plant NO_x emissions. A plot of O_3 versus NO_y is similar to that of O_3 versus NO_x [*Liu et al.*, 1987; *Milford et al.*, 1989, 1994; *McKeen et al.*, 1991; *Sillman*, 1995].

[44] Figure 8 shows the 21 July 2000 UTC differences in WRF-Chem [NO_y] and [O_3] between the 2003 perturbation and 1999 reference emission inventory cases, ΔNO_y and ΔO_3, averaged over the lowest 1 km of the model. Above approximately 1 km the impact of changes in E(NO_x) decreases drastically with increasing altitude. The plumes

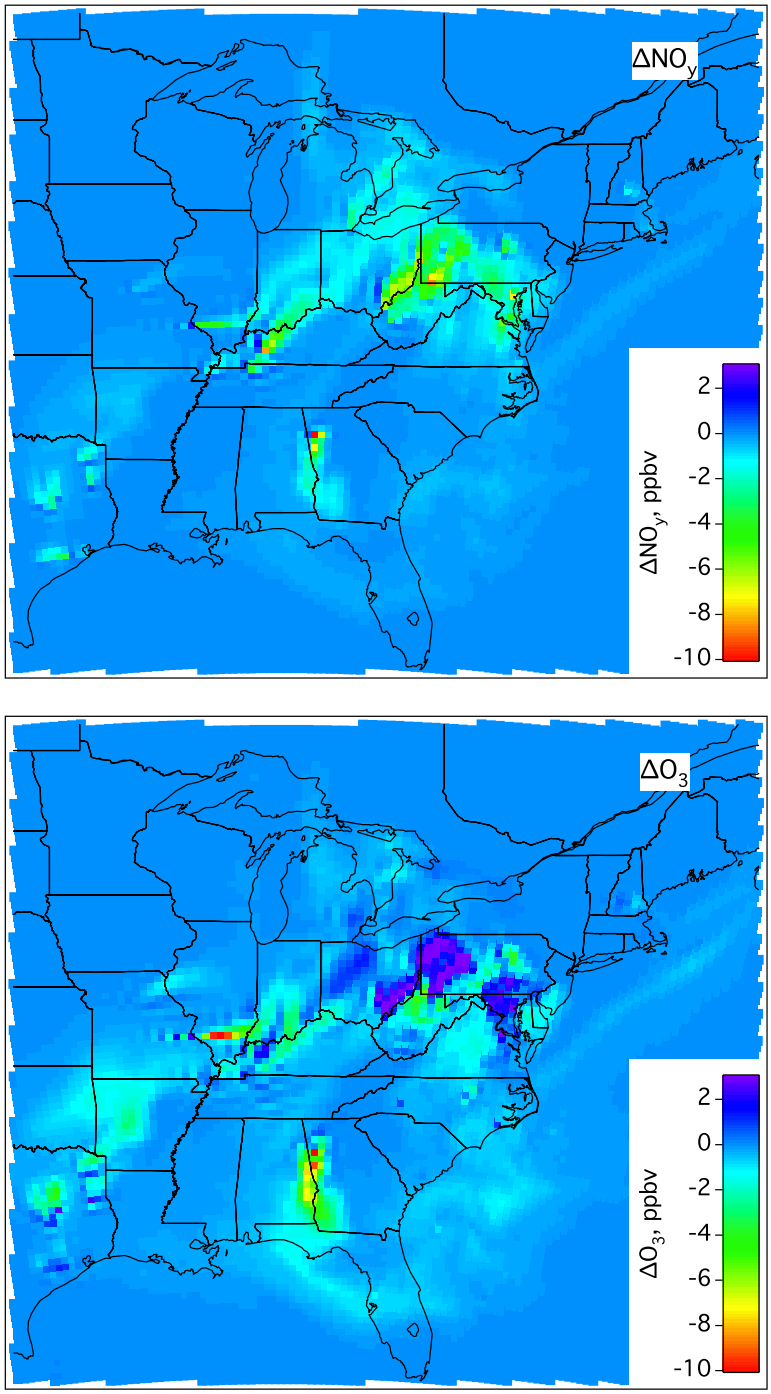

Figure 8. WRF-Chem perturbation – reference emission inventory case differences in the mixing ratios of (top) NO_y and (bottom) O_3 averaged over the lowest 1 km of the simulation domain at 2000 UTC on 21 July 2004. The equivalent ΔNO_y and ΔO_3 color scales saturate at both ends of the range for better contrast. Maximum/minimum values: ΔNO_y = 1.6/−14.4 ppbv, ΔO_3 = 4.8/−10.9 ppbv.

of plants with the largest reductions in E(NO_x) appear as NO_y decreases of up to 14 ppbv, equivalent to about 60% of a reference case [NO_y] = 22 ppbv. In response to the E(NO_x) reductions, O_3 has absolute decreases comparable to or larger than the reductions in NO_y in some plumes while other plumes have small O_3 increases. The maximum O_3 decrease in response to emission reductions is 14% of a reference case O_3 mixing ratio of almost 80 ppbv.

[45] Plumes from individual perturbation plants, or groups of plants in close proximity to each other, are isolated using the following procedure (Figure 9). Model grid cells affected by plumes from plants with NO_x emission changes have nonzero ΔNO_y, i.e., the difference in NO_y between the perturbation and reference EI cases. ΔNO_y can therefore be used to distinguish cells with perturbation plant contributions from cells affected by other sources.

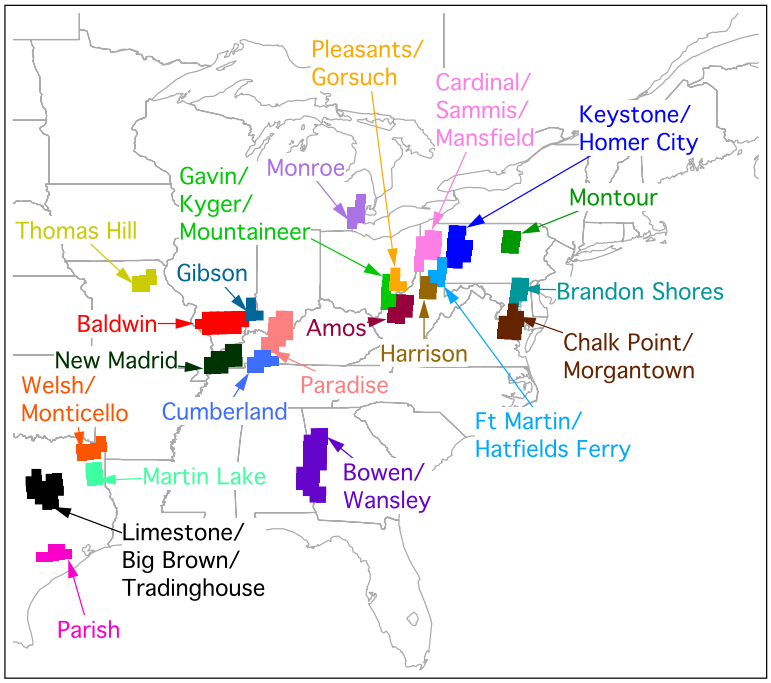

Figure 9. The 0–1 km averages of model grid cells affected by plumes from individual perturbation plants or groups of closely located plants from the WRF-Chem simulations at 2000 UTC on 21 July 2004, isolated using the procedures described in the text.

Grid cells with power plant contributions also have elevated NO_y and SO_2, while cells with urban influence show simultaneous enhancements in NO_y and CO. Cells with a significant combination of power plant plume and urban impacts are excluded from this analysis. Rather than using exact concentration limits to determine each plume's extent, the above indicators are used in a qualitative way to isolate only those cells with primarily power plant influence.

[46] Grid cells assigned to particular plumes are also characterized by O_3 which correlates well with $NO_z = NO_y - NO_x$. The slope of the linear portion of the O_3 versus NO_z curve, defined as the ozone production efficiency (OPE), represents the amount of O_3 molecules produced per NO_x molecule emitted [*Liu et al.*, 1987; *Lin et al.*, 1988; *Trainer et al.*, 1993; *Hirsch et al.*, 1996; *Ryerson et al.*, 1998, 2001, 2003; *Nunnermacker et al.*, 2000; *Sillman*, 2000; *Zaveri et al.*, 2003]. NO_x emissions are instantly diluted in the model's 27 km × 27 km grid cells, causing model NO_x levels to be lower than in a true plume and leading to higher OPEs than those derived from correlations of observed mixing ratios in an actual plume [*Sillman*, 2000; *Zaveri et al.*, 2003]. OPEs derived from correlations of O_3 versus NO_z, whether simulated or observed, are also affected by dry deposition of HNO_3 (O_3 deposits more slowly than HNO_3), and will therefore tend to be upper limits to the true ozone production efficiency. Nonetheless, as demonstrated below, the model OPEs exhibit the correct relative trends with respect to plume NO_x levels, VOC availability, and solar flux.

[47] Figure 10 displays the perturbation – reference EI differences ΔO_3 versus ΔNO_y for all grid cells and for the isolated perturbation plant plumes identified in Figure 9. The largest decreases in model O_3 on the afternoon of 21 July result from E(NO_x) decreases in the plumes of Baldwin (Figure 10a) and Bowen/Wansley (Figure 10b). These plumes approach a limiting decrease of 6 moles of O_3 per mole of decreased NO_x emissions. Other plumes with similar behavior on 21 July include Gibson, New Madrid, Limestone/Big Brown/Tradinghouse, Martin Lake, and Welsh/Monticello. At the other extreme are plumes, such as those from Keystone/Homer City (Figure 10b) and Cardinal/Sammis/Mansfield (Figure 10a), in which a decrease of 1 mole of emitted NO_x results in an increase of 1 mole of O_3. Plumes having general O_3 increases, with ΔO_3 versus ΔNO_y slopes between 0 and −1, are associated with Gavin/Kyger Creek/Mountaineer, Pleasants/Gorsuch, Fort Martin/Hatfields Ferry, Chalk Point/Morgantown, Brandon Shores, and Parish. The remaining plumes (Paradise, Cumberland, Thomas Hill, Amos, Harrison, Monroe, and Montour) show intermediate behavior of smaller O_3 decreases or increases within these two extremes. On other days in the 3-week study period, the range of ΔO_3 and ΔNO_y is similar to that shown in Figure 10 for 21 July. 21 July has more plant plumes with large negative ΔO_3 values compared with other days because more plants were under clear skies throughout the afternoon. An analogous plot to Figure 10 for other days may have a different arrangement of plumes from the specific plants, for the reasons described in the next paragraph.

[48] The variable effects of NO_x emission reductions on O_3 are a result of whether the plume is in a relatively lower NO_x or higher NO_x regime, because of the characteristic nonlinear dependence of O_3 on NO_x. At lower NO_x the plume chemistry favors conversion of NO to NO_2 by peroxy radicals, leading to enhanced production rates and yields of ozone. At higher NO_x, radical loss primarily

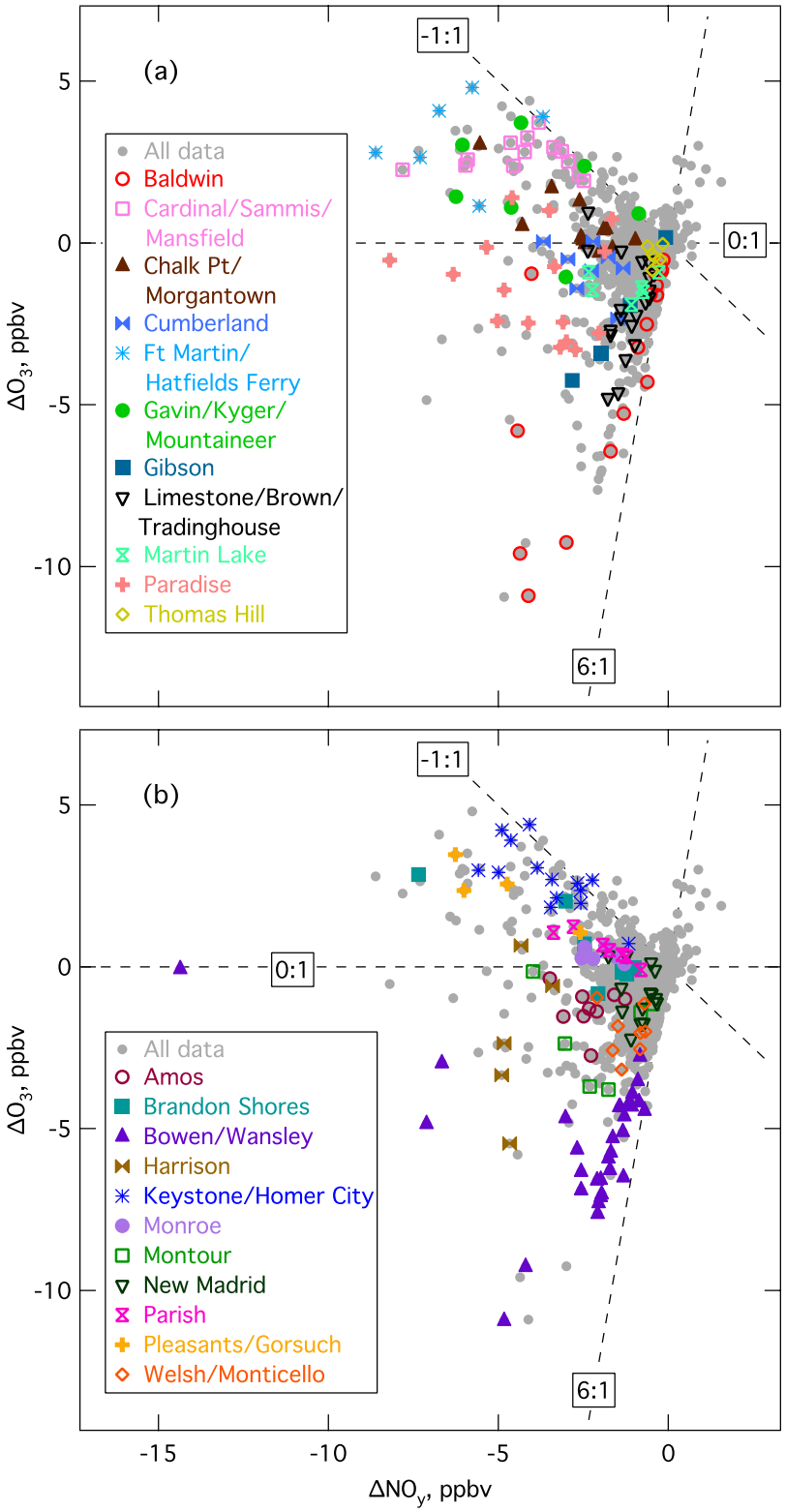

Figure 10. (a and b) WRF-Chem perturbation – reference case differences ΔO_3 versus ΔNO_y for all grid cells (gray circles) and for the isolated plant plumes shown in Figure 9 (colored symbols). The 22 isolated plumes are shown in either Figure 10a or 10b for clarity. For reference, the dotted black lines indicate slopes of 6, 0, and −1 ppbv ΔO_3 per ppbv ΔNO_y. All data are at 2000 UTC on 21 July 2004 and are averaged over the lowest 1 km of the simulation domain.

through OH + NO_2 and titration of O_3 by NO result in lower ozone levels. The precise shape of the O_3 – NO_x dependence, the location of the turnover point, and consequently the regime a specific plume is in on a particular day depend on a number of factors, including the strength of the plant's NO_x emissions, how fast the plume disperses, [NO_x] in the air into which the plume is emitted, the availability of sunlight, and VOC emissions (often from biogenic sources in the plumes considered here) that mix in to the plume during its advection and dispersion. These effects have been discussed extensively in modeling and observational investigations of power plant plumes [*Nunnermacker et al.*, 2000; *Sillman*, 2000; *Ryerson et al.*, 1998, 2001, 2003; *Luria et al.*, 2000, 2003] and in more general studies of the dependence of tropospheric O_3 on NO_x and VOCs [*Liu et al.*, 1987; *Lin et al.*, 1988; *McKeen et al.*, 1991; *Trainer et al.*, 1993; *Milford et al.*, 1989, 1994; *Sillman*, 1995; *Jacob et al.*, 1995; *Hirsch et al.*, 1996; *Zaveri et al.*, 2003; *Reynolds et al.*, 2004; *Kleinman*, 2005]. The wide range of O_3 changes resulting from power plant E(NO_x) decreases seen in the WRF-Chem simulations are expected because of the large variability in each of these controlling parameters across the model domain.

[49] We present a brief comparison of two plumes that lie at the extremes of Figure 10 to qualitatively illustrate these effects. Figure 11 compares the Baldwin and Keystone/Homer City (KHC) plumes on 21 July at 2000 UTC in terms of O_3 versus NO_y and O_3 versus NO_z for the reference and perturbation EI cases and perturbation – reference differences ΔO_3 versus ΔNO_y. Baldwin represents plumes in Figure 10 for which decreases in NO_x emissions cause even larger decreases in O_3. On the afternoon of 21 July the Baldwin plume is in a region isolated from other large NO_x sources (Figures 6–9). It has strong photochemical activity due to high biogenic emissions and clear skies. The reference and perturbation EI cases of the Baldwin plume have similar O_3 versus NO_z curves with large (≈5) slopes (Figure 11a). In both EI cases this plume lies almost exclusively to the low NO_y side of the O_3 versus NO_y turnover point (Figure 11b). Reducing E(NO_x) shifts the plume to lower O_3. The maximum amount of the O_3 decrease between the perturbation and reference cases is described by the OPE, and in the ΔO_3 versus ΔNO_y plot (Figure 11c) most of the Baldwin plume data approach the OPE limiting line with a slope of 5.

[50] The KHC plume on 21 July is characteristic of the upper limit in Figure 10 in which decreasing NO_x results in increasing O_3. On the afternoon of 21 July, the KHC plume is under cloudy skies, which dampen calculated biogenic

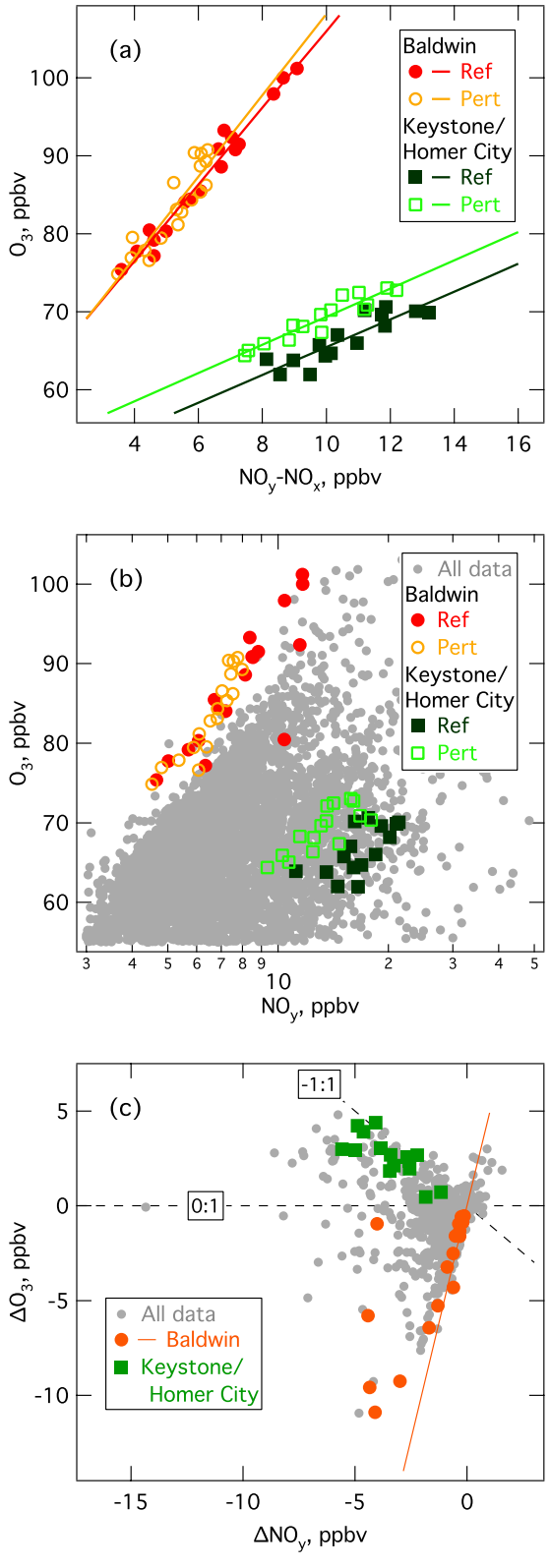

Figure 11. WRF-Chem simulation data at 2000 UTC on 21 July 2004 and averaged over the lowest 1 km. See Figure 9 for the locations of plumes referred to in Figure 11. (a) O_3 versus NO_y-NO_x for grid cells within the Baldwin and Keystone/Homer City plumes for the reference (solid symbols) and perturbation (open symbols) cases and linear fits (lines) to these data. (b) O_3 versus NO_y for a subset of all grid cells in the reference case (gray dots) and for grid cells within the Baldwin and Keystone/Homer City plumes for the reference (colored solid symbols) and perturbation (colored open symbols) cases. (c) ΔO_3 versus ΔNO_y for the difference between the perturbation and reference cases in all grid cells (gray dots, data same as gray circles shown in Figure 10) and for grid cells within the Baldwin and Keystone/Homer City plumes (colored symbols). The orange line with slope = 4.9 represents the Baldwin O_3 production efficiency in the reference case.

VOC emissions and photochemical activity in comparison with the Baldwin plume. KHC total NO_x emissions are 25% less than those of Baldwin. However, KHC emissions entered more NO_x-rich air than the Baldwin plume, since on 21 July KHC lies downwind of numerous other power plants along the Ohio River (Figures 6–9). The KHC plume correspondingly has a much smaller OPE (slope of O_3 versus NO_z curve $\approx$ 1.8) than Baldwin (Figure 11a). The KHC perturbation case O_3 versus NO_z curve is shifted to higher O_3 than that for the reference case, reflecting the elevated background O_3 in the perturbation case. Net O_3 titration occurs under the higher NO_x conditions of this plume, so that O_3 is higher by 1 mole for every mole that NO_x emissions decrease (Figures 11b and 11c).

4. Conclusions

[51] Summertime NO_x emission rates measured by CEMS at a collection of 53 eastern U.S. power plants dropped by about 50% between 1999 and 2003, while SO_2 emission rates at most of the same plants decreased only marginally during the same period. CEMS E(SO_2)/E(NO_x) data from 2003 and 2004 agree with 2004 observations of the SO_2/NO_{yi} ratio made by the NOAA WP-3 aircraft in the plumes of many of these plants. WRF-Chem model simulations using the NEI99 and an inventory in which the emission rates of these 53 power plants were updated to 2003 summer levels demonstrate the impact of NO_x emission reductions during a July day in 2004. In response to decreases in power plant NO_x emissions, modest decreases in O_3 are observed in some plumes while small O_3 increases occur in others.

[52] The precise change in modeled ozone resulting from power plant NO_x emission reductions is a complex interaction of the plant's NO_x emissions, levels of NO_x in the air in to which the plume is emitted, VOC emissions in the vicinity of the plant, and sunlight availability. The changes in O_3 predicted by WRF-Chem in response to the NO_x emission reductions are consistent with many previous studies and are not surprising. Generally speaking, a given decrease in E(NO_x) at low levels of NO_y reduces O_3, while at higher NO_y levels the same E(NO_x) decrease results in a smaller O_3 decrease or even an O_3 increase. This behavior is a direct consequence of the nonlinear dependence of O_3 on NO_x. In order to achieve the same decreases in photochemically produced O_3, plants with large E(NO_x) or those located in regions of high ambient [NO_x] (such as near population centers or within dense concentrations of point sources) will require more extensive NO_x emission reductions than plants with lower NO_x emissions or those in more isolated areas. Local VOC emissions and meteorology also play a role in the effect of a given reduction in NO_x emissions. Plumes evolving with higher actinic flux or larger biogenic VOC emissions will remain in the ozone-producing regime at higher NO_x levels than those in less photochemically active regions, modulating the day-to-day impacts of emission reductions at a particular plant.

[53] Model-simulated O_3 impacts of power plant E(NO_x) reductions during the summer of 2004 are not large most likely because of the meteorological conditions. Since prolonged stagnation events were relatively absent that summer, there were few opportunities for plumes to build upon the previous day's emissions and create high O_3 concentrations. Instead, the effects of power plant emission reductions are geographically discrete, apparent locally during the day of emission but rapidly diminishing by the following day as plumes disperse under strong flow conditions. However, the model simulations demonstrate that in plumes from plants relatively isolated from other large NO_x sources and in photochemically active areas, molar O_3 decreases per mole of decreased NO_x emissions can be large, even in a relatively cool summer. In a year with more typical conditions, including sustained multiday pollution episodes, NO_x emission reductions at many eastern U.S. power plants are expected to have more significant impacts than were seen in 2004.

[54] Assuming the trend in the emissions of the 53 perturbation plants studied in this work applies to all eastern U.S. coal-burning plants, summertime power plant E(NO_x) is overestimated by approximately a factor of two in current air quality model inventories based on the NEI99. The NEI99 also does not capture the seasonal variation of power plant NO_x emissions, since ozone season E(NO_x) < 25% of annual E(NO_x) when recent pollution controls are considered. These model input errors will continue for the near future if the current multiyear EPA inventory preparation period persists. For example, the final version of the 1999 NEI was not available until March 2004, a lag of nearly 5 years. One possible improvement that would facilitate merging CEMS data with the NEI would be the use of a common format to identify power generation units and to allocate emissions to each unit. Another step EPA could take to expedite the delivery of new NEI versions is to separate the power plant portion from the rest of the inventory, instead of combining all point sources in one data set. A new power plant NEI could then be released in yearly or even quarterly updates as new CEMS data become available.

[55] The current study is only an initial assessment of air quality impacts resulting from recent emission changes. A more complete study requires updating the NO_x emissions of all U.S. power plants using the latest available CEMS data followed by model simulations to assess the impact of these emission changes on O_3. To remove daily fluctuations due to meteorology and quantify regional impacts on O_3 resulting from these emission changes, simulations should be carried out for longer time periods and monthly and seasonal statistics examined. Because of the coarse grid resolution of WRF-Chem relative to the scale of the power plant plumes and the lack of a plume-in-grid treatment, some caution must be used in interpreting simulated changes in plume O_3 in response to E(NO_x) reductions. Comparisons of the model results to aircraft observations made during NEAQS2K4 and previous field experiments and to data from surface O_3 monitoring networks would also be useful.

[56] Power plants account for a large fraction of NO_x emissions in particular regions of the United States, such as the Ohio River valley (where power plants are $\sim$50% of total NO_x emissions). Surface monitors and targeted field studies must be located in areas where the most significant trends in power plant emissions and their resulting impacts are expected to occur, in order to maximize the probability of detecting these changes. Whereas aircraft observations

and surface monitoring networks may be able to detect local changes in nitrogen and ozone levels, satellite observations will likely be needed to quantify large-scale and long-term differences. As a result of recent pollution controls, power plants now represent a smaller fraction of total U.S. NO_x emissions than they did in the past several decades. The transportation sector is likely to have an increasingly greater impact on ozone levels than electric power generation. Accurate quantification of NO_x and VOC emissions from mobile sources and trends in these emissions are critical [*Parrish et al.*, 2002; *Parrish*, 2006; *Harley et al.*, 2005; http://www.epa.gov/ttn/chief/trends/index.html].

References

Butler, T. J., G. E. Likens, F. M. Vermeylen, and B. J. B. Stunder (2005), The impact of changing nitrogen oxide emissions on wet and dry nitrogen deposition in the northeastern USA, *Atmos. Environ.*, *39*, 4851–5862.

Erisman, J. W., A. van Pul, and P. Wyers (1994), Parameterization of surface resistance for the quantification of atmospheric deposition of acidifying pollutants and ozone, *Atmos. Environ.*, *28*, 2595–2607.

Grell, G. A., S. Emeis, W. R. Stockwell, T. Schoenemeyer, R. Forkel, J. Michalakes, R. Knoche, and W. Seidl (2000), Application of a multiscale, coupled MM5/chemistry model to the complex terrain of the VOTALP valley campaign, *Atmos. Environ.*, *34*, 1435–1453.

Grell, G. A., S. E. Peckham, R. Schmitz, S. A. McKeen, G. Frost, W. C. Skamarock, and B. Eder (2005), Fully coupled "online" chemistry within the WRF model, *Atmos. Environ.*, *39*, 6957–6975.

Harley, R. A., L. C. Marr, J. K. Lehner, and S. N. Giddings (2005), Changes in motor vehicle emissions on diurnal to decadal time scales and effects on atmospheric composition, *Environ. Sci. Technol.*, *39*, 5356–5362.

Hirsch, A. I., J. W. Munger, D. J. Jacob, L. W. Horowitz, and A. H. Goldstein (1996), Seasonal variation of the ozone production efficiency per unit NO_x at Harvard Forest, Massachusetts, *J. Geophys. Res.*, *101*, 12,659–12,666.

Jacob, D. J., L. W. Horowitz, J. W. Munger, B. G. Heikes, R. R. Dickerson, R. S. Artz, and W. C. Keene (1995), Seasonal transition from NO_{x-} to hydrocarbon-limited conditions for ozone production over the eastern United States in September, *J. Geophys. Res.*, *100*(D5), 9315–9324.

Kleinman, L. I. (2005), The dependence of tropospheric ozone production rate on ozone precursors, *Atmos. Environ.*, *39*, 575–586.

Lin, X., M. Trainer, and S. C. Liu (1988), On the nonlinearity of tropospheric ozone production, *J. Geophys. Res.*, *93*, 15,879–15,888.

Liu, S. C., M. Trainer, F. C. Fehsenfeld, D. D. Parrish, E. J. Williams, D. W. Fahey, G. Hübler, and P. C. Murphy (1987), Ozone production in the rural troposphere and the implications for regional and global ozone distributions, *J. Geophys. Res.*, *92*, 4191–4207.

Luria, M., R. L. Tanner, R. E. Imhoff, R. J. Valente, E. M. Bailey, and S. F. Mueller (2000), Influence of natural hydrocarbons on ozone formation in an isolated power plant plume, *J. Geophys. Res.*, *105*, 9177–9188.

Luria, M., R. E. Imhoff, R. J. Valente, and R. L. Tanner (2003), Ozone yields and production efficiencies in a large power plant plume, *Atmos. Environ.*, *37*, 3593–3603.

Madronich, S. (1987), Photodissociation in the atmosphere: 1. Actinic flux and the effects of ground reflections and clouds, *J. Geophys. Res.*, *92*, 9740–9752.

McKeen, S. A., E.-Y. Hsie, and S. C. Liu (1991), A study of the dependence of rural ozone on ozone precursors in the eastern United States, *J. Geophys. Res.*, *96*, 15,377–15,394.

McKeen, S., et al. (2005), Assessment of an ensemble of seven real-time ozone forecasts over eastern North America during the summer of 2004, *J. Geophys. Res.*, *110*, D21307, doi:10.1029/2005JD005858.

Milford, J. B., A. G. Russell, and G. J. McRae (1989), A new approach to photochemical pollution control: Implications of spatial patterns in pollutant responses to reductions in nitrogen oxides and reactive organic gas emissions, *Environ. Sci. Technol.*, *23*, 1290–1301.

Milford, J. B., D. Gao, S. Sillman, P. Blossey, and A. G. Russell (1994), Total reactive nitrogen (NO_y) as an indicator of the sensitivity of ozone to reductions in hydrocarbon and NO_x emissions, *J. Geophys. Res.*, *99*, 3533–3542.

Neuman, J. A., et al. (2002), Fast-response airborne in situ measurements of HNO_3 during the Texas 2000 Air Quality Study, *J. Geophys. Res.*, *107*(D20), 4436, doi:10.1029/2001JD001437.

Neuman, J. A., D. D. Parrish, T. B. Ryerson, C. A. Brock, C. Wiedinmyer, G. J. Frost, J. S. Holloway, and F. C. Fehsenfeld (2004), Nitric acid loss rates measured in power plant plumes, *J. Geophys. Res.*, *109*, D23304, doi:10.1029/2004JD005092.

Nunnermacker, L. J., L. I. Kleinman, D. Imre, P. H. Daum, Y.-N. Lee, J. H. Lee, S. R. Springston, L. Newman, and N. Gillani (2000), NO_y lifetimes and O_3 production efficiencies in urban and power plant plumes: Analysis of field data, *J. Geophys. Res.*, *105*, 9165–9176.

Parrish, D. D. (2006), Critical evaluation of US on-road vehicle emission inventories, *Atmos. Environ.*, *40*, 2288–2300, doi:10.1016/j.atmosenv.2005.11.033.

Parrish, D. D., M. Trainer, D. Hereid, E. J. Williams, K. J. Olszyna, R. A. Harley, J. F. Meagher, and F. C. Fehsenfeld (2002), Decadal change in carbon monoxide to nitrogen oxide ratio in U.S. vehicular emissions, *J. Geophys. Res.*, *107*(D12), 4140, doi:10.1029/2001JD000720.

Placet, M., C. O. Mann, R. O. Gilbert, and M. J. Niefer (2000), Emissions of ozone precursors from stationary sources: A critical review, *Atmos. Environ.*, *34*, 2183–2204.

Reynolds, S. D., C. L. Blanchard, and S. D. Ziman (2004), Understanding the effectiveness of precursor reductions in lowering 8-hr ozone concentrations—Part II. The eastern United States, *J. Air Waste Manage. Assoc.*, *54*, 1452–1470.

Ryerson, T. B., et al. (1998), Emissions lifetimes and ozone formation in power plant plumes, *J. Geophys. Res.*, *103*, 22,569–22,583.

Ryerson, T. B., L. G. Huey, K. Knapp, J. A. Neuman, D. D. Parrish, D. T. Sueper, and F. C. Fehsenfeld (1999), Design and initial characterization of an inlet for gas-phase NO_y measurements from aircraft, *J. Geophys. Res.*, *104*, 5483–5492.

Ryerson, T. B., E. J. Williams, and F. C. Fehsenfeld (2000), An efficient photolysis system for fast-response NO_2 measurements, *J. Geophys. Res.*, *105*, 26,447–26,461.

Ryerson, T. B., et al. (2001), Observations of ozone formation in power plant plumes and implications for ozone control strategies, *Science*, *292*, 719–723.

Ryerson, T. B., et al. (2003), Effect of petrochemical industrial emissions of reactive alkenes and NO_x on tropospheric ozone formation in Houston, Texas, *J. Geophys. Res.*, *108*(D8), 4249, doi:10.1029/2002JD003070.

Sillman, S. (1995), The use of NO_y, H_2O_2, and HNO_3 as indicators for ozone-NO_x-hydrocarbon sensitivity in urban locations, *J. Geophys. Res.*, *100*, 14,175–14,188.

Sillman, S. (2000), Ozone production efficiency and loss of NO_x in power plant plumes: Photochemical model and interpretation of measurements in Tennessee, *J. Geophys. Res.*, *105*, 9189–9202.

Slinn, S. A., and W. G. N. Slinn (1980), Prediction for particle deposition on natural waters, *Atmos. Environ.*, *14*, 1013–1016.

Slusher, D. L., L. G. Huey, D. J. Tanner, F. Flocke, and J. M. Roberts (2004), A TD-CIMS technique for the simultaneous measurement of peroxyacyl nitrates and dinitrogen pentoxide, *J. Geophys. Res.*, *109*, D19315, doi:10.1029/2004JD004670.

Stockwell, W. R., P. Middleton, J. S. Chang, and X. Tang (1990), The second generation regional acid deposition model chemical mechanism for regional air quality modeling, *J. Geophys. Res.*, *95*, 16,343–16,367.

Stockwell, W. R., F. Kirchner, M. Kuhn, and S. Seefeld (1997), A new mechanism for regional atmospheric chemistry modeling, *J. Geophys. Res.*, *102*, 25,847–25,879.

Swanson, A. L., F. Flocke, J. Roberts, G. Huey, D. Tanner, J. Orlando, G. Tyndall, and D. Hanson (2004), Characterization of a TD-CIMS instrument for aircraft measurements of PeroxyAcetyl Nitrate (PAN) compounds, *Eos Trans. AGU*, *85*(47), Fall Meet. Suppl., Abstract A42B-04.

Trainer, M., et al. (1993), Correlation of ozone with NO_y in photochemically aged air, *J. Geophys. Res.*, *98*, 2917–2925.

U.S. Environmental Protection Agency (2003), Acid Rain Program 2002 progress report, *Rep. EPA-430-R-03-011*, Clean Air Markets Div., Off. of Air and Radiat., Washington, D. C. (Available at http://www.epa.gov/airmarkets/cmprpt/arp02/index.html)

U.S. Environmental Protection Agency (2004a), Acid Rain Program 2003 progress report, *Rep. EPA-430-R-04-009*, Clean Air Markets Div., Off. of Air and Radiat., Washington, D. C. (Available at http://www.epa.gov/airmarkets/cmprpt/arp03/summary.html)

U.S. Environmental Protection Agency (2004b), NO_x Budget Trading Program 2003 progress and compliance report, *Rep. EPA-430-R-04-010*, Clean Air Markets Div., Off. of Air and Radiat., Washington, D. C. (Available at http://www.epa.gov/airmarkets/fednox/index.html)

U.S. Environmental Protection Agency (2004c), The ozone report: Measuring progress through 2003, *Rep. EPA-454/K-04-001*, Emissions, Monit., and Anal. Div., Off. of Air Qual. Planning and Stand., Research Triangle Park, N. C. (Available at http://www.epa.gov/airtrends/ozone.html)

Wesley, M. L. (1989), Parameterization of surface resistance to gaseous dry deposition in regional numerical models, *Atmos. Environ.*, *16*, 1293–1304.

Zaveri, R. A., C. M. Berkowitz, L. I. Kleinman, S. R. Springston, P. V. Doskey, W. A. Lonneman, and C. W. Spicer (2003), Ozone production efficiency and NO_x depletion in an urban plume: Interpretation of field

observations and implications for evaluating O_3-NO_x-VOC sensitivity, *J. Geophys. Res.*, *108*(D14), 4436, doi:10.1029/2002JD003144.

N. Auerbach, J. Cartwright, T. Habermann, and D. Kowal, NOAA National Geophysical Data Center, Boulder, CO 80305, USA.

F. C. Fehsenfeld, T. Fortin, G. J. Frost, J. S. Holloway, S. A. McKeen, J. A. Neuman, D. D. Parrish, J. M. Roberts, T. B. Ryerson, D. T. Sueper, A. Swanson, and M. Trainer, Chemical Sciences Division, Earth System Research Laboratory, NOAA, Boulder, CO 80305, USA. (gregory.j.frost@noaa.gov)

F. Flocke, Atmospheric Chemistry Division, National Center for Atmospheric Research, Boulder, CO 80307, USA.

G. A. Grell and S. E. Peckham, Global Systems Division, Earth System Research Laboratory, NOAA, Boulder, CO 80305, USA.